SIAM J. SCI. COMPUT.
Vol. 20, No. 3, pp. 781–810

ASYMPTOTIC SOLUTION OF STIFF PDEs WITH THE CSP METHOD: THE REACTION DIFFUSION EQUATION*

M. HADJINICOLAOU† AND D. A. GOUSSIS†

Abstract. The computational singular perturbation (CSP) method is employed for the solution of stiff PDEs and for the acquisition of the most important physical understanding. The usefulness of the method is demonstrated by analyzing a transient reaction-diffusion problem. It is shown that in the regions where the solution exhibits smooth spatial slopes, a simple nonstiff system of equations can be used instead of the full governing equations. From the simplified system, which is numerically provided by CSP and whose structure varies with space and time, important physical information comes to light. The relation of this method to the class of asymptotic expansion methods is explored. It is shown that the CSP results are identical to the ones obtained by the asymptotic methods. The identifications of the nondimensional parameters and the tedious manipulations needed by the asymptotic methods are performed by programmable numerical or analytic computations specified by CSP. Preliminary numerical results are presented validating the theoretical aspects of the proposed algorithm and providing a measure of its usefulness and its accuracy.

Key words. asymptotic expansions, stiff PDEs, order reduction

AMS subject classifications. 41A60, 65M12, 76V05

1. Introduction.

A large number of physical phenomena (in fluid dynamics, combustion, control, chemical kinetics, etc.) are characterized by a large number of unknowns and a wide range of temporal or spatial scales. These scales are encountered in the governing differential equations and create serious numerical difficulties (stiffness) when the numerical solution is sought. In physical terms, these phenomena are driven by different physical processes at different points in time or space. In general, each such process is characterized by a different scale. As a result, at each instant the behavior of the phenomenon's evolution depends on the kind of driving process involved. For example, when fast or slow processes are dominant, the solution undergoes a fast or slow, respectively, transient. However, fast and slow scales are present in the dynamics of the problem, independently of whether the driving processes are fast or slow. Stiffness arises when the characteristic scale of the solution is slower than the scale of the fastest processes. Such an occurence means that the fastest processes have reached an equilibrium creating some constraints which the solution must satisfy. Usually, the existence of such constraints has a physical explanation. In complex numerical simulations, gaining the physical understanding is equally significant with computing the numerical solution. Such physical insight includes the identification of the important or unimportant processes, parameters, and unknowns in the problem, etc. In order to address the issues of both stiffness and physical understanding, a variety of asymptotic methods have been developed which explore the existing disparity in scales [1, 2, 3]. The goal of all these techniques is the generation of a simple and nonstiff mathematical model which captures all important features of the processes in the problem under consideration. However, since these techniques involve extensive analytical work (identification of the proper nondimensional parameters, the gauge functions, etc.) and require experience and intuition, they can be used only when the system of differential equations governing the physical problem is simple and small.

*Received by the editors May 16, 1996; accepted for publication (in revised form) July 8, 1997; published electronically October 7, 1998.
http://www.siam.org/journals//sisc/20-3/30399.html
†Mechanical Engineering Department, University of Patras, 26110 Rio-Patras, Greece (dagoussi@iceht.forth.gr, hadjini@thermo.mech.upatras.gr).

Here we shall consider a stiff reaction-diffusion system of differential equations, the stiffness of which is created mainly by the source term. For this kind of problem, the outcome of a conventional asymptotic analysis is a simple nonstiff system accompanied by a sequence of steady-state and/or partial equilibrium approximations [4, 5, 6]. The conditions under which these approximations are valid are never known a priori. Their justification requires experience and physical insight. Specifically, the implementation of the steady state approximation requires the identification of the unknowns which are likely to reach quasi-steady behavior. On the other hand, the partial equilibrium approximation requires the identification of processes that are fast and that are likely to become partially equilibrated. Given a stiff problem, the decision on which approximation is appropriate must be made by the investigator before knowing the solution. Such a decision is based on the introduction of the proper scaling for the dependent and independent parameters and the identification of a small parameter. In addition, the investigator must properly use these approximations in order to simplify the problem by tedious paper-and-pencil manipulations. When the stiff system of equations under consideration is large and complex, these approximations are difficult to identify, justify, and apply.

Here, we shall demonstrate that the computational singular perturbation (CSP) method can perform everything the asymptotic methods can, with no limits imposed by the size and complexity of the problem at hand. The CSP method was first developed for the solution of stiff ODEs in the context of initial value problems [7, 8, 9, 10]. Here, the applicability of the method is extended to stiff PDEs. The methodology for producing a simplified nonstiff system of PDEs with CSP will be presented, and the conditions under which such a simplification is feasible will be stated. In particular, a reaction-diffusion problem will be analyzed by both analytic asymptotic methods and CSP. Two sets of input parameters are considered which allow the use of the steady-state and partial equilibrium approximations, respectively. The difficulties encountered when using the conventional asymptotic methods will be demonstrated. On the other hand, it will be shown that when using the CSP method for analytical or numerical operations, the correct approximations are obtained with a simple algorithm and the simplified nonstiff equations are automatically derived.

The structure of the manuscript is as follows. First, the reaction-diffusion problem shall be defined and analyzed by conventional asymptotics. Then, the CSP method will be introduced and extended for the general form of the reaction-diffusion problem. Both analytical and numerical results obtained with the CSP method will be presented and compared with those obtained on the basis of the conventional asymptotics and the original system of equations.

2. Formulation of the problem. We consider a reaction-diffusion process described by a system of differential equations which in general form can be written

$$\frac{\partial \mathbf{y}}{\partial t} = \mathbf{L}(\mathbf{y}) + \mathbf{g}(\mathbf{y}), \tag{1}$$

where $\mathbf{y}$ is the N-dimensional vector of unknowns, $\mathbf{L}$ is the diffusion differential vector operator, and $\mathbf{g}$ is an N-dimensional nonlinear function representing the source term. To proceed, it is assumed that this system is stiff, and in particular we assume that the stiffness is mainly caused by the source term $\mathbf{g}$. As is expected in this case, some of the eigenvalues of the Jacobian of $\mathbf{g}$ have negative and large-in-magnitude real part, while the remaining eigenvalues are relatively small.

Here, we shall analyze the classical chain-reaction mechanism considered first by Trotman-Dickenson [11]. The full chemical kinetics mechanism consists of the following four elementary reactions:

$$\text{(2a)} \qquad \text{Initiation:} \qquad M_1 \overset{\kappa_1}{\rightarrow} R_1 + M_2;$$

$$\text{(2b)} \qquad \text{Propagation:} \qquad R_1 + M_1 \overset{\kappa_2}{\rightarrow} R_1 H + R_2,$$

$$\text{(2c)} \qquad R_2 \overset{\kappa_3}{\rightarrow} R_1 + M_3;$$

$$\text{(2d)} \qquad \text{Termination:} \qquad R_1 + R_2 \overset{\kappa_4}{\rightarrow} M_4,$$

where κ_1, κ_2, κ_3, and κ_4 are the reaction rate constants of the four elementary reactions. Considering a simple model of an isothermal and one-dimensional imperfectly stirred reactor, the governing system of equations is as follows:

$$\text{(3a)} \qquad \frac{\partial R_1}{\partial t} = \alpha_1 D^2 R_1 + \kappa_1 M_1 - \kappa_2 R_1 M_1 + \kappa_3 R_2 - \kappa_4 R_1 R_2,$$

$$\text{(3b)} \qquad \frac{\partial R_2}{\partial t} = \alpha_2 D^2 R_2 + \kappa_2 R_1 M_1 - \kappa_3 R_2 - \kappa_4 R_1 R_2,$$

$$\text{(3c)} \qquad \frac{\partial M_1}{\partial t} = \alpha_3 D^2 M_1 - \kappa_1 M_1 - \kappa_2 R_1 M_1,$$

where R_1, R_2, and M_1 are concentrations, α_1, α_2, and α_3 are diffusion coefficients, x is the spatial coordinate, and $D = \partial/\partial x$. Referring to the original equation (1), the components of the vector $\mathbf{y}$ are R_1, R_2, M_1, the differentials $\alpha_1 D^2$, $\alpha_2 D^2$, and $\alpha_3 D^2$ are the elements of the diffusion operator $\mathbf{L}(\mathbf{y})$, and the function $\mathbf{g}(\mathbf{y})$ is defined as:

$$\text{(4)} \qquad \mathbf{g} = \mathbf{S}_1 F^1 + \mathbf{S}_2 F^2 + \mathbf{S}_3 F^3 + \mathbf{S}_4 F^4,$$

where the stoichiometric vectors $\mathbf{S}_i$ and the reaction rates F^i are the columns of the matrix $\mathbf{S}$ and the elements of the vector $\mathbf{F}$, respectively:

$$\text{(5)} \qquad \mathbf{S} = \begin{bmatrix} 1 & -1 & 1 & -1 \\ 0 & 1 & -1 & -1 \\ -1 & -1 & 0 & 0 \end{bmatrix}, \qquad \mathbf{F} = \begin{bmatrix} k_1 M_1 \\ k_2 R_1 M_1 \\ k_3 R_2 \\ k_4 R_1 R_2 \end{bmatrix}.$$

We consider the boundary conditions:

$$\text{(6a)} \qquad R_1(x=0) = 0, \quad R_2(x=0) = 0, \quad M_1(x=0) = 1,$$

$$\text{(6b)} \qquad DR_1(x=L) = 0, \quad DR_2(x=L) = 0, \quad DM_1(x=L) = 0,$$

which indicate that at $x = 0$ the fuel M_1 diffuses in and the products R_1 and R_2 diffuse out. At $x = L$ a physical boundary exists that prevents anything from crossing.

When some of the reaction rate constants κ_1, κ_2, κ_3, and κ_4 are large, stiffness causes serious difficulties in obtaining the numerical solution of the system of equations (3a)–(3c). The conventional procedure to overcome this problem is to use asymptotic expansions. Such methods have already been employed for the analysis of (3a)–(3c) in the absence of the differential aperator D^2 [12]. Some of the difficulties arising when applying this procedure are presented in the section that follows.

3. Conventional asymptotics. We consider the case where:

(i) the initiation reaction (2a) is much slower than the propagation reaction (2b), so that $\kappa_1 \ll \kappa_2$, and

(ii) the propagation reaction (2b) is much slower than the termination reaction (2d), so that $\kappa_2 \ll \kappa_4$.

On the basis of these assumptions, we introduce the following scaling for the concentrations, time and space [12]:

$$y_1 = \frac{\kappa_2}{\kappa_1 K} R_1, \quad y_2 = \frac{2\kappa_4 K}{\kappa_2} R_2, \quad y_3 = M_1, \quad \tau = \kappa_1 K t, \quad z = \frac{x}{L}, \tag{7}$$

where

$$K = \frac{1}{4} + \frac{1}{4}\left(1 + \frac{1}{\nu}\right)^{1/2}, \qquad \nu = \frac{\kappa_1 \kappa_4}{8\kappa_2 \kappa_3}, \tag{8}$$

and L is the length of the spatial computational domain. With this scaling, the governing equations (3a–3c) become:

$$\frac{\partial y_1}{\partial \tau} = q_1 E^2 y_1 + \frac{\omega_1}{K}\left(\frac{y_3}{K} - y_1 y_3 + \frac{y_2}{2cK} - \frac{y_1 y_2}{2K}\right), \tag{9a}$$

$$\frac{\partial y_2}{\partial \tau} = q_2 E^2 y_2 + 2K\omega_2\left(y_1 y_3 - \frac{y_2}{2cK} - \frac{y_1 y_2}{2K}\right), \tag{9b}$$

$$\frac{\partial y_3}{\partial \tau} = q_3 E^2 y_3 + \left(-\frac{y_3}{K} - y_1 y_3\right), \tag{9c}$$

where

$$\omega_1 = \frac{\kappa_2}{\kappa_1}, \quad \omega_2 = \frac{\kappa_4}{\kappa_2}, \quad c = \frac{1}{2K - 1} = 8\nu K, \tag{10a}$$

$$q_1 = \frac{\alpha_1}{\kappa_1 K L^2}, \quad q_2 = \frac{\alpha_2}{\kappa_1 K L^2}, \quad q_3 = \frac{\alpha_3}{\kappa_1 K L^2}, \tag{10b}$$

and $E = \partial/\partial z$. Given that κ_1 and κ_2 are assumed to be much smaller than κ_2 and κ_4, respectively, it follows that:

$$\omega_1 \gg 1, \qquad \omega_2 \gg 1. \tag{11}$$

For simplicity, we will assume that both ω_1 and ω_2 are of the same order (i.e., $\omega_1 = O(\omega_2)$). Using the expressions (10a) for ω_1 and ω_2, the relation (8) defining ν becomes

$$\nu = \frac{1}{8}\frac{\omega_2}{\omega_1}\frac{\kappa_2}{\kappa_3}. \tag{12}$$

Since ω_1 and ω_2 were assumed to be of the same order, it follows that the value of ν is proportional to the ratio κ_2/κ_3. Next it will be shown that the value of this ratio determines the asymptotic behavior of the solution of the system of equations (3a)–(3c).

3.1. The steady-state approximation. First we consider the case where $\kappa_2 \gg \kappa_3$. It can be easily shown that in this case, $\nu \gg 1$ and $K = O(1)$. Therefore, since ω_1 and ω_2 were assumed to be much larger than $O(1)$, in the domain where the time and space derivatives are all $O(1)$ (i.e., the stiffness is caused by the source terms), equations (9a)–(9c) are simplified to:

$$0 \approx \frac{y_3}{K} - y_1 y_3 + \frac{y_2}{2cK} - \frac{y_1 y_2}{2K}, \tag{13a}$$

$$0 \approx y_1 y_3 - \frac{y_2}{2cK} - \frac{y_1 y_2}{2K}, \tag{13b}$$

$$\frac{\partial y_3}{\partial \tau} = q_3 E^2 y_3 + \left(-\frac{y_3}{K} - y_1 y_3\right). \tag{13c}$$

These results show that, on the basis of the assumptions denoted by (11) and for $\kappa_2/\kappa_3 \gg 1$, the original system of the three differential equations (9a)–(9c) reduces to the steady-state relations (13a)–(13b) for y_1 and y_2 and the differential equation (13c) for y_3. Solving the two algebraic equations (13a)–(13b) for y_1 and y_2 and substituting in the differential equation (13c) yields:

$$y_1 \approx 1, \tag{14a}$$

$$y_2 \approx y_3, \tag{14b}$$

$$\frac{\partial y_3}{\partial \tau} \approx q_3 E^2 y_3 - 3y_3. \tag{14c}$$

As was mentioned above, the asymptotic solution to the original problem produced by (14a)–(14c) is valid when $\nu \gg 1$. It is easy to show that the same asymptotic equations are obtained in the case where ν is of $O(1)$. A different approximation is derived next.

3.2. The partial equilibrium approximation. In the case where $\kappa_2/\kappa_3 \ll 1$, then $\nu \ll 1$. In the limit of $\nu \to 0$, the parameters K and c tend to the following limiting values:

$$K \to \frac{1}{4\sqrt{\nu}}, \qquad c \to 2\sqrt{\nu}, \tag{15}$$

which indicates that the scaling given by (7) is no more valid. For this case, the proper scaling for the concentrations, time and space, is as follows:

$$y_1 = \sqrt{\frac{\kappa_2}{\kappa_1}} R_1, \quad y_2 = \kappa_3 \sqrt{\kappa_1} R_2, \quad y_3 = \kappa_1 \sqrt{\kappa_2} M_1, \quad \tau = \sqrt{\kappa_1 \kappa_2}\, t, \quad z = \frac{x}{L}. \tag{16}$$

Using this scaling, the governing equations (3a)–(3c) become

$$\frac{\partial y_1}{\partial \tau} = p_1 E^2 y_1 + \chi(y_3 - 8\nu\omega_1 y_1 y_2) - \chi\sqrt{\omega_1}(y_1 y_3 - y_2), \tag{17a}$$

$$\frac{\partial y_2}{\partial \tau} = p_2 E^2 y_2 + (-\omega_2 y_1 y_2) + \frac{\omega_2}{8\nu\sqrt{\omega_1}}(y_1 y_3 - y_2), \tag{17b}$$

$$\frac{\partial y_3}{\partial \tau} = p_3 E^2 y_3 + \left(-\frac{y_3}{\sqrt{\omega_1}} - y_1 y_3\right), \tag{17c}$$

where

$$p_1 = \frac{\alpha_1}{\sqrt{\kappa_1\kappa_2}L^2}, \quad p_2 = \frac{\alpha_2}{\sqrt{\kappa_1\kappa_2}L^2}, \quad p_3 = \frac{\alpha_3}{\sqrt{\kappa_1\kappa_2}L^2}, \quad \chi = \frac{1}{\kappa_1\sqrt{\kappa_2}}. \tag{18}$$

Since ω_1 and ω_2 were assumed to be much larger than unity, in the domain where the time and space derivatives are all of $O(1)$, the differential equations (17a)–(17b) produce in the $\nu \to 0$ limit:

$$y_1 y_3 \approx y_2, \tag{19}$$

which is the partial equilibrium approximation for the two propagation reactions (2b)–(2c). In this case, the simplified set of equations is not obtained by simply substituting (19) into the governing equations (17a)–(17c). The proper procedure is as follows.

Differentiating (19) with respect to time, substituting from (17a)–(17c) and solving for $(y_1y_3 - y_2)$ we obtain

$$(y_1y_3 - y_2) \approx Q\Bigg[y_3p_1E^2y_1 - p_2E^2y_2 + y_1p_3E^2y_3 - y_1\left(\frac{y_3}{\sqrt{\omega_1}} + y_1y_3\right) + \omega_2y_1y_2 + \chi y_3(y_3 - 8\nu\omega_1y_1y_2)\Bigg], \tag{20}$$

where

$$Q = \left[\frac{8\nu\sqrt{\omega_1}}{\omega_2 + 8\nu\chi\omega_1y_3}\right].$$

In the limit of $\nu \to 0$, (20) produces (19). First substituting (20) in (17a)–(17c) and then taking the limit $\nu \to 0$, we obtain with respect to the leading order:

$$\frac{\partial y_1}{\partial \tau} \approx p_1E^2y_1 + \chi y_3, \tag{21a}$$

$$\frac{\partial y_2}{\partial \tau} \approx y_3p_1E^2y_1 + y_1p_3E^2y_3 + \chi y_3y_3 - y_1y_1y_3, \tag{21b}$$

$$\frac{\partial y_3}{\partial \tau} \approx p_3E^2y_3 - y_1y_3. \tag{21c}$$

Given the algebraic relation (19) and the three differential equations (21a)–(21c), the choice of the three equations forming the simplified system is not easy. It will be shown later that it consists of the algebraic relation (19) and the two differential equations (21a) and (21c).

3.3. Remarks. Apart from an initial short transient and a short region near $x = 0$, the solution of the system of differential equations (3a)–(3c) is smooth. As a result, the two simplified systems derived for the two cases $\nu \gg 1$ and $\nu \ll 1$ can replace the original system (3a)–(3c) in most of the computational domain providing good accuracy. The significance of the simplified systems is based on the fact that their numerical solution exhibits no computational difficulties due to stiffness. Consequently, a larger time step and a coarser grid than the one used for the original system can be used. However, as was made clear from the simple system treated above, producing such nonstiff simplified systems is not an easy task. Specifically, for the problem at hand and for the two limiting cases considered, it was shown that two different kinds of scalings had to be defined and the appropriate limits had to be taken. Furthermore, for deriving the simplified system the resulting algebraic equations had to be used in a specific manner involving a large amount of analytical work. Obviously, for the treatment of any other limiting case, similar steps must be followed. Since such a procedure cannot be carried out if the problem under consideration is large and complex, an algorithmic method for deriving simplified systems is of great importance. Such a method has already been developed for the case of a scalar equation and when there is only temporal stiffness, due to both the spatial operator and the source term [13]. In the next paragraph we shall present a general method which is algorithmic and is not limited by the complexity or size of the problem.

4. The CSP method. The CSP method was first developed for the solution of initial value problems of ODEs in which there exists a vast disparity of time scales. Given a system of N ODEs, the CSP method is based on the appropriate split of

the N-dimensional space of the unknowns $\mathbf{y}$ in two subspaces [7, 8, 9, 10]. The first (fast) subspace consists of those vectors that correspond to the largest eigenvalues of the Jacobian of $\mathbf{g}$. The negligible projection of $\mathbf{g}$ to this subspace provides algebraic relations among all the unknowns. The second (slow) subspace consists of the vectors that correspond to the remaining small eigenvalues of the Jacobian of $\mathbf{g}$. The projection of $\mathbf{g}$ to this subspace produces the simplified nonstiff problem. Here, the applicability of the CSP method shall be extended for problems in the general form of the reaction-diffusion equation (1), in the case where the stiffness is introduced mainly by the source term $\mathbf{g}$.

Let us assume that the basis vectors spanning the space of $\mathbf{y}$ are the set of N-dimensional column vectors $\mathbf{a}_i$ $(i = 1, N)$ which are partitioned as:

$$\mathbf{a}_r = [\mathbf{a}_1, \mathbf{a}_2, \ldots, \mathbf{a}_M], \qquad \mathbf{a}_s = [\mathbf{a}_{M+1}, \mathbf{a}_{M+2}, \ldots, \mathbf{a}_N]. \tag{22}$$

The dual basis consists of N-dimensional row vectors $\mathbf{b}^i$ $(i = 1, N)$, which are partitioned as:

$$\mathbf{b}^r = \begin{bmatrix} \mathbf{b}^1 \\ \mathbf{b}^2 \\ \vdots \\ \mathbf{b}^M \end{bmatrix}, \qquad \mathbf{b}^s = \begin{bmatrix} \mathbf{b}^{M+1} \\ \mathbf{b}^{M+2} \\ \vdots \\ \mathbf{b}^N \end{bmatrix}, \tag{23}$$

where, by definition,

$$\mathbf{b}^r\mathbf{a}_r = \mathbf{I}, \quad \mathbf{b}^r\mathbf{a}_s = \mathbf{0}, \quad \mathbf{b}^s\mathbf{a}_r = \mathbf{0}, \quad \mathbf{b}^s\mathbf{a}_s = \mathbf{I}. \tag{24}$$

The scalar M which is a function of both space and time denotes the number of time scales that are faster in comparison to the "locally" dominant (characteristic) scale. It is assumed that the M vectors in $\mathbf{a}_r$ span the fast subspace of $\mathbf{y}$, while the $N - M$ vectors in $\mathbf{a}_s$ span the slow subspace. We rewrite (1) as:

$$\frac{\partial \mathbf{y}}{\partial t} = \mathbf{a}_r\mathbf{h}^r + \mathbf{a}_s\mathbf{h}^s, \tag{25}$$

where

$$\mathbf{h}^r = \mathbf{b}^r(\mathbf{L} + \mathbf{g}), \qquad \mathbf{h}^s = \mathbf{b}^s(\mathbf{L} + \mathbf{g}). \tag{26}$$

At any point in time and space, the CSP-produced basis vectors guarantee that the M amplitudes in $\mathbf{h}^r$ are negligible:

$$h^i = \mathbf{b}^i \cdot (\mathbf{L} + \mathbf{g}) \approx 0, \quad i = 1, M. \tag{27}$$

Therefore, the system of differential equations (25) becomes

$$\frac{\partial \mathbf{y}}{\partial t} \approx \mathbf{a}_s\mathbf{h}^s. \tag{28}$$

Equation (27) indicates that the projection of the vector $\mathbf{L} + \mathbf{g}$ on the M vectors $\mathbf{b}^i$ $(i = 1, M)$ is negligible. A more clear picture of its significance can be obtained if we consider the case where $\mathbf{g}$ consists of K additive terms:

$$\mathbf{g} = \mathbf{SF} = [\mathbf{S}_1\mathbf{S}_2 \ldots \mathbf{S}_K] \begin{bmatrix} F^1 \\ F^2 \\ \vdots \\ F^K \end{bmatrix} = \mathbf{S}_1F^1 + \mathbf{S}_2F^2 + \cdots + \mathbf{S}_KF^K, \tag{29}$$

where $\mathbf{S}_i$ are N-dimensional column vectors and F^i are scalars. In that case, (27) becomes

$$h^i = \mathbf{b}^i \cdot \mathbf{L} + B_1^i F^1 + B_2^i F^2 + \cdots + B_K^i F^K \approx 0, \quad i = 1, M, \tag{30}$$

where

$$B_j^i = \mathbf{b}^i \cdot \mathbf{S}_j. \tag{31}$$

It is seen that the negligible value of h^i is the product of significant cancellations among the $K + 1$ terms in the right-hand side of (30). If we assume that the term $\mathbf{b}^i \cdot \mathbf{L}$ does not contribute much in the occurring cancellations, (30) simplifies to

$$f^i = \mathbf{b}^i \cdot \mathbf{g} = B_1^i F^1 + B_2^i F^2 + \cdots + B_K^i F^K \approx 0, \quad i = 1, M, \tag{32}$$

which express the equilibrium relations among the different physical processes in the source term $\mathbf{g}$. The M algebraic equations (32) can be solved for M specific elements of $\mathbf{y}$ indicated by the CSP pointer [9, 10]. Specifically, the M diagonal elements of the matrix $\mathbf{a}_r \mathbf{b}^r$ that are closest to unity identify the corresponding elements in the vector of the unknowns $\mathbf{y}$ which can be determined by the M algebraic relations (32).

When the N-dimensional simplified system of differential equations (28) and the M algebraic relations (32) are available, the asymptotic solution can be obtained with two different procedures. The first one consists of solving the simplified N differential equations in (28) by discretizing in space the right-hand side and integrating in time. According to this procedure, at each time step the "homogeneous correction" [9, 10]

$$\mathbf{y}_k^n \leftarrow \mathbf{y}_k^n - (\mathbf{a}_r \tau_r^r \mathbf{f}^r)_k^n \tag{33}$$

must be applied, where the superscript n refers to the time step, the subscript k refers to the space discretization, and $\boldsymbol{\tau}_r^r$ and $\mathbf{f}^r$ are defined as

$$\boldsymbol{\tau}_r^r = (\mathbf{b}^r \mathbf{J} \mathbf{a}_r)^{-1}, \qquad \mathbf{f}^r = \mathbf{b}^r \mathbf{g},$$

where $\mathbf{J}$ is the Jacobian of $\mathbf{g}$. This correction ensures that the algebraic equations (32) are satisfied to leading order as the integration of (28) proceeds in time.

Alternatively, the second procedure for obtaining the asymptotic solution is to solve the M algebraic equations (32) and $N - M$ differential equations. This is achieved as follows. Let us assume that the vector of the unknowns $\mathbf{y}$ is partitioned as $\mathbf{y} = [\mathbf{u}^T, \mathbf{w}^T]$, where $\mathbf{u}$ and $\mathbf{w}$ are M and $N - M$ dimensional vectors respectively. The M components of $\mathbf{y}$ in $\mathbf{u}$ are the ones pointed to by the CSP pointer, while the $N - M$ components in $\mathbf{w}$ are the remaining components of $\mathbf{y}$. According to these definitions, (28) can be cast as

$$\frac{\partial}{\partial t} \begin{bmatrix} \mathbf{u} \\ \mathbf{w} \end{bmatrix} \approx \begin{bmatrix} \mathbf{a}_{us} \\ \mathbf{a}_{ws} \end{bmatrix} \mathbf{h}^s, \tag{34}$$

where

$$\mathbf{a}_s = \begin{bmatrix} \mathbf{a}_{us} \\ \mathbf{a}_{ws} \end{bmatrix}.$$

The simplified system consists of the $N - M$ differential equations:

$$\frac{\partial \mathbf{w}}{\partial t} \approx \mathbf{a}_{ws} \mathbf{h}^s \tag{35}$$

and the M algebraic relations (32):

$$f^i(\mathbf{u};\mathbf{w}) = B_1^i F^1 + B_2^i F^2 + \cdots + B_K^i F^K \approx 0, \quad i = 1, M. \tag{36}$$

The usefulness of this simplified system of equations is twofold. First, the system of differential equations (28) is nonstiff so that a large time step can be used. This is guaranteed by the absence of the fast component $\mathbf{a}_r \mathbf{h}^r$ of the original right-hand side $\mathbf{L} + \mathbf{g}$. In addition, since only $N - M$ components of (28) are used, the number of unknowns to be discretized is smaller than those in the original equation. The overall efficiency for obtaining the approximate solution of the reaction-diffusion problem described by (1) is the outcome of the speedup produced by the larger time step and the smaller number of unknowns and the slowdown caused by the additional computations required for the computation of the basis vectors.

5. The CSP basis vectors. The procedure for determining the appropriate basis vectors for the reaction-diffusion problem, given by (1), through which the simplified system of differential equations (28) and the algebraic relations (32) are produced, is developed as follows. Let us assume that there exist an arbitrary set of N-dimensional basis vectors which are partitioned as in (22), i.e., $\mathbf{a}_{or}$ and $\mathbf{a}_{os}$. For simplicity, we assume that these vectors are constant (i.e., time and space independent). The corresponding dual basis vectors are denoted by $\mathbf{b}^{or}$ and $\mathbf{b}^{os}$, partitioned as in (23). Under the assumption that the stiffness of (1) is mainly caused by the source term $\mathbf{g}$, it is expected that the Jacobian of $\mathbf{g}$ produces a number, say M, of eigenvalues that have negative and large-in-magnitude real part. At each point in time and space, we can define the small parameter ε:

$$\varepsilon = \frac{|\mu(M+1)|}{|\mu(M)|}, \tag{37}$$

where $\mu(i)$ is the ith eigenvalue of the Jacobian of $\mathbf{g}$. Since $\mathbf{g}$ is a function of space and time, $\mu(i)$ and ε are also functions of space and time. The parameter ε is a measure of the stiffness of the problem, since M denotes the number of fast time scales.

Expanding $\mathbf{g}$ on the basis of $\mathbf{a}_{or}$ and $\mathbf{a}_{os}$, (1) yields

$$\frac{\partial \mathbf{y}}{\partial t} = \mathbf{L} + \mathbf{a}_{or}\mathbf{f}^{or} + \mathbf{a}_{os}\mathbf{f}^{os}, \tag{38}$$

where

$$\mathbf{f}^{or} = \mathbf{b}^{or}\mathbf{g}, \qquad \mathbf{f}^{os} = \mathbf{b}^{os}\mathbf{g}. \tag{39a,b}$$

The amplitudes $\mathbf{f}^{or}$ and $\mathbf{f}^{os}$ (fast and slow, respectively) are governed by the following differential equations:

$$\frac{\partial \mathbf{f}^{or}}{\partial t} = \boldsymbol{\lambda}_{or}^{or}\mathbf{f}^{or} + \boldsymbol{\lambda}_{os}^{or}\mathbf{f}^{os} + \mathbf{b}^{or}\mathbf{J}\mathbf{L} \tag{40a}$$

$$\frac{\partial \mathbf{f}^{os}}{\partial t} = \boldsymbol{\lambda}_{or}^{os}\mathbf{f}^{or} + \boldsymbol{\lambda}_{os}^{os}\mathbf{f}^{os} + \mathbf{b}^{os}\mathbf{J}\mathbf{L}, \tag{40b}$$

where $\mathbf{J}$ is the Jacobian of $\mathbf{g}$ and

$$\boldsymbol{\lambda}_{or}^{or} = \mathbf{b}^{or}\mathbf{J}\mathbf{a}_{or}, \qquad \boldsymbol{\lambda}_{os}^{or} = \mathbf{b}^{or}\mathbf{J}\mathbf{a}_{os}, \tag{41a}$$

$$\boldsymbol{\lambda}_{or}^{os} = \mathbf{b}^{os}\mathbf{J}\mathbf{a}_{or}, \qquad \boldsymbol{\lambda}_{os}^{os} = \mathbf{b}^{os}\mathbf{J}\mathbf{a}_{os}. \tag{41b}$$

Since the vectors in $\mathbf{b}^{or}$ and $\mathbf{b}^{os}$ are orthogonal to the vectors in $\mathbf{a}_{or}$ and $\mathbf{a}_{os}$, the $N \times N$ matrix $\boldsymbol{\lambda}_o$ defined as

$$\boldsymbol{\lambda}_o = \begin{bmatrix} \boldsymbol{\lambda}_{or}^{or} & \boldsymbol{\lambda}_{os}^{or} \\ \boldsymbol{\lambda}_{or}^{os} & \boldsymbol{\lambda}_{os}^{os} \end{bmatrix} \tag{42}$$

is similar to the matrix $\mathbf{J}$. Note that when $\mathbf{L} = \mathbf{0}$, the governing equations for the amplitudes $\mathbf{f}^{or}$ and $\mathbf{f}^{os}$ reduce to those developed for the homogeneous problem [9, 10].

Given the constant sets of vectors $\mathbf{a}_{or}$, $\mathbf{a}_{os}$, $\mathbf{b}^{or}$, and $\mathbf{b}^{os}$, the CSP basis vectors $\mathbf{a}_r$, $\mathbf{a}_s$, $\mathbf{b}^r$, and $\mathbf{b}^s$ (used in the presentation of the CSP method in section 4) are produced as follows.

5.1. The a_r and b^s vectors. Let us first consider (40b), which governs the evolution of the slow amplitudes $\mathbf{f}^{os}$:

$$\frac{\partial \mathbf{f}^{os}}{\partial t} = \boldsymbol{\lambda}_{or}^{os}\mathbf{f}^{or} + \boldsymbol{\lambda}_{os}^{os}\mathbf{f}^{os} + \mathbf{b}^{os}\mathbf{JL}. \tag{40b}$$

Due to the first term $\boldsymbol{\lambda}_{or}^{os}\mathbf{f}^{or}$ on the right-hand side of (40b), there is mode mixing between the fast and slow amplitudes. This mixing becomes unimportant when the norm of the matrix $\boldsymbol{\lambda}_{or}^{os}$ becomes sufficiently small. In order to define the appropriate basis vectors which produce such a matrix, we proceed as follows. Solving (40a) with respect to $\mathbf{f}^{or}$ we obtain:

$$\mathbf{f}^{or} = \boldsymbol{\tau}_{or}^{or}\frac{\partial \mathbf{f}^{or}}{\partial t} - \boldsymbol{\tau}_{or}^{or}\boldsymbol{\lambda}_{os}^{or}\mathbf{f}^{os} - \boldsymbol{\tau}_{or}^{or}\mathbf{b}^{or}\mathbf{JL}, \tag{43}$$

where

$$\boldsymbol{\tau}_{or}^{or} = (\boldsymbol{\lambda}_{or}^{or})^{-1}. \tag{44}$$

Substituting the expression (43) in (40b) yields

$$\frac{\partial \mathbf{f}^{os}}{\partial t} = \boldsymbol{\lambda}_{or}^{os}\left(\boldsymbol{\tau}_{or}^{or}\frac{\partial \mathbf{f}^{or}}{\partial t} - \boldsymbol{\tau}_{or}^{or}\boldsymbol{\lambda}_{os}^{or}\mathbf{f}^{os} - \boldsymbol{\tau}_{or}^{or}\mathbf{b}^{or}\mathbf{JL}\right) + \boldsymbol{\lambda}_{os}^{os}\mathbf{f}^{os} + \mathbf{b}^{os}\mathbf{JL}. \tag{45}$$

Rearranging, we obtain:

$$\begin{aligned} \frac{\partial}{\partial t}(\mathbf{f}^{os} - \boldsymbol{\lambda}_{or}^{os}\boldsymbol{\tau}_{or}^{or}\mathbf{f}^{or}) = -\frac{\partial}{\partial t}(\boldsymbol{\lambda}_{or}^{os}\boldsymbol{\tau}_{or}^{or})\mathbf{f}^{or} + (\boldsymbol{\lambda}_{os}^{os} - \boldsymbol{\lambda}_{or}^{os}\boldsymbol{\tau}_{or}^{or}\boldsymbol{\lambda}_{os}^{or})\mathbf{f}^{os} \\ + (\mathbf{b}^{os} - \boldsymbol{\lambda}_{or}^{os}\boldsymbol{\tau}_{or}^{or}\mathbf{b}^{or})\mathbf{JL}. \end{aligned} \tag{46}$$

Equation (46) suggests that a new set of slow amplitudes can be defined as

$$\mathbf{f}^{s} = \mathbf{f}^{os} - \boldsymbol{\lambda}_{or}^{os}\boldsymbol{\tau}_{or}^{or}\mathbf{f}^{or}. \tag{47}$$

Equation (47) implies that, relative to the old amplitudes $\mathbf{f}^{os}$, the new amplitudes $\mathbf{f}^{s}$ are to leading order free of a fast component. Using (39b), this new set of slow amplitudes can also be obtained if the following new set of vectors $\mathbf{b}^{s}$ were introduced:

$$\mathbf{b}^{s} = \mathbf{b}^{os} - \boldsymbol{\lambda}_{or}^{os}\boldsymbol{\tau}_{or}^{or}\mathbf{b}^{or} = \mathbf{b}^{os}[\mathbf{I} - \mathbf{a}_r\mathbf{b}^{or}], \tag{48}$$

where the set of vectors $\mathbf{a}_r$ is defined as

$$\mathbf{a}_r = \mathbf{a}_{or} + \mathbf{a}_{os}\boldsymbol{\lambda}_{or}^{os}\boldsymbol{\tau}_{or}^{or} = \mathbf{J}\mathbf{a}_{or}\boldsymbol{\tau}_{or}^{or}. \tag{49}$$

The new set of basis vectors consisting of $\mathbf{a}_r$ and $\mathbf{a}_{os}$ is orthogonal to the set of vectors in $\mathbf{b}^{or}$ and $\mathbf{b}^s$:

$$\mathbf{b}^{or}\mathbf{a}_r = \mathbf{I}, \quad \mathbf{b}^{or}\mathbf{a}_{os} = \mathbf{0}, \quad \mathbf{b}^s\mathbf{a}_r = \mathbf{0}, \quad \mathbf{b}^s\mathbf{a}_{os} = \mathbf{I}. \tag{50}$$

Using the expressions for the new slow modes $\mathbf{f}^s$, (46) becomes

$$\begin{aligned}\frac{\partial \mathbf{f}^s}{\partial t} = &\left[-\frac{\partial}{\partial t}(\boldsymbol{\lambda}^{os}_{or}\boldsymbol{\tau}^{or}_{or}) + (\boldsymbol{\lambda}^{os}_{os} - \boldsymbol{\lambda}^{os}_{or}\boldsymbol{\tau}^{or}_{or}\boldsymbol{\lambda}^{or}_{os})\boldsymbol{\lambda}^{os}_{or}\boldsymbol{\tau}^{or}_{or}\right]\mathbf{f}^{or} \\ &+ (\boldsymbol{\lambda}^{os}_{os} - \boldsymbol{\lambda}^{os}_{or}\boldsymbol{\tau}^{or}_{or}\boldsymbol{\lambda}^{or}_{os})\mathbf{f}^s + (\mathbf{b}^{os} - \boldsymbol{\lambda}^{os}_{or}\boldsymbol{\tau}^{or}_{or}\mathbf{b}^{or})\mathbf{JL}\end{aligned} \tag{51}$$

or

$$\frac{\partial \mathbf{f}^s}{\partial t} = \boldsymbol{\lambda}^s_r\mathbf{f}^{or} + \boldsymbol{\lambda}^s_{os}\mathbf{f}^s + \mathbf{b}^s\mathbf{JL}, \tag{52}$$

where

$$\boldsymbol{\lambda}^s_{os} = \left(\frac{\partial \mathbf{b}^s}{\partial t} + \mathbf{b}^s\mathbf{J}\right)\mathbf{a}_{os} = \mathbf{b}^s\mathbf{J}\mathbf{a}_{os} = \boldsymbol{\lambda}^{os}_{os} - \boldsymbol{\lambda}^{os}_{or}\boldsymbol{\tau}^{or}_{or}\boldsymbol{\lambda}^{or}_{os}, \tag{53}$$

$$\boldsymbol{\lambda}^s_r = \left(\frac{\partial \mathbf{b}^s}{\partial t} + \mathbf{b}^s\mathbf{J}\right)\mathbf{a}_r = -\frac{\partial}{\partial t}(\boldsymbol{\lambda}^{os}_{or}\boldsymbol{\tau}^{or}_{or}) + \boldsymbol{\lambda}^s_s\boldsymbol{\lambda}^{os}_{or}\boldsymbol{\tau}^{or}_{or}. \tag{54}$$

The advantage of the set of basis vectors in $\mathbf{a}_r$ and $\mathbf{a}_{os}$ and their dual in $\mathbf{b}^{or}$ and $\mathbf{b}^s$ can be appreciated if the original and transformed equations for the slow amplitudes $\mathbf{f}^{os}$ and $\mathbf{f}^s$, equations (40b) and (52) respectively, are compared. The norm of the matrix $\boldsymbol{\lambda}^s_r$ is by $O(\varepsilon)$ smaller than the norm of the matrix $\boldsymbol{\lambda}^{os}_{or}$ and the eigenvalues of the matrix $\boldsymbol{\lambda}^s_{os}$ are $O(\mu(M+1))$ [14]. This is achieved if the initial vectors in $\mathbf{a}_{or}$ and $\mathbf{b}^{or}$ have a component in the fast subspace in $\mathbf{J}$ and its dual [14]. With the new set of vectors, the mode mixing between the fast and slow amplitudes decreases and, if the magnitude of $\mathbf{f}^{or}$ is sufficiently small, the slow modes evolve with the slow time scales.

With the new set of basis vectors $\mathbf{a}_r$ and $\mathbf{a}_{os}$ and their dual $\mathbf{b}^{or}$ and $\mathbf{b}^s$, (38) becomes

$$\frac{\partial \mathbf{y}}{\partial t} = \mathbf{L} + \mathbf{a}_r\mathbf{f}^{or} + \mathbf{a}_{os}\mathbf{f}^s, \tag{55}$$

where

$$\mathbf{f}^{or} = \mathbf{b}^{or}\mathbf{g}, \qquad \mathbf{f}^s = \mathbf{b}^s\mathbf{g}. \tag{56}$$

The fast modes now evolve according to the equation

$$\frac{\partial \mathbf{f}^{or}}{\partial t} = \boldsymbol{\lambda}^{or}_r\mathbf{f}^{or} + \boldsymbol{\lambda}^{or}_{os}\mathbf{f}^s + \mathbf{b}^{or}\mathbf{JL}, \tag{57}$$

where

$$\boldsymbol{\lambda}^{or}_r = \mathbf{b}^{or}\mathbf{J}\mathbf{a}_r, \qquad \boldsymbol{\lambda}^{or}_{os} = \mathbf{b}^{or}\mathbf{J}\mathbf{a}_{os}. \tag{58}$$

5.2. The b^r and a_s vectors. Let us now consider (57) governing the evolution of the fast amplitudes $\mathbf{f}^{or}$, which is now cast in the form

$$\frac{\partial \mathbf{f}^{or}}{\partial t} = \boldsymbol{\lambda}_r^{or}(\mathbf{f}^{or} + \boldsymbol{\tau}_r^{or}\boldsymbol{\lambda}_{os}^{or}\mathbf{f}^s + \boldsymbol{\tau}_r^{or}\mathbf{b}^{or}\mathbf{JL}), \tag{59}$$

where

$$\boldsymbol{\tau}_r^{or} = (\boldsymbol{\lambda}_r^{or})^{-1}. \tag{60}$$

Since the new basis vectors $\mathbf{a}_r$ are now used, the M eigenvalues of the $M \times M$ matrix $\boldsymbol{\lambda}_r^{or}$ are leading order approximations of the M eigenvalues of $\mathbf{J}$ which are large and have negative real parts (accuracy of $O(\varepsilon)$ [14]). Therefore, $\mathbf{f}^{or}$ will exponentially approach an asymptotic value defined by

$$\mathbf{f}_\infty^{or} = -\boldsymbol{\tau}_r^{or}\boldsymbol{\lambda}_{os}^{or}\mathbf{f}^s - \boldsymbol{\tau}_r^{or}\mathbf{b}^{or}\mathbf{JL}. \tag{61}$$

Wishing to make the fast amplitudes $\mathbf{f}^{or}$ as fast as possible (i.e., to decay exponentially and become insignificant), we subtract from $\mathbf{f}^{or}$ its asymptotic value so that (55) becomes

$$\frac{\partial \mathbf{y}}{\partial t} = \mathbf{L} + \mathbf{a}_r(\mathbf{f}^{or} - \mathbf{f}_\infty^{or}) + \mathbf{a}_r\mathbf{f}_\infty^{or} + \mathbf{a}_{os}\mathbf{f}^s. \tag{62}$$

Noticing that

$$\begin{aligned}
\mathbf{f}^{or} - \mathbf{f}_\infty^{or} &= \mathbf{b}^{or}\mathbf{g} + \boldsymbol{\tau}_r^{or}\boldsymbol{\lambda}_{os}^{or}\mathbf{b}^s\mathbf{g} + \boldsymbol{\tau}_r^{or}\mathbf{b}^{or}\mathbf{JL} \\
&= (\mathbf{b}^{or} + \boldsymbol{\tau}_r^{or}\boldsymbol{\lambda}_{os}^{or}\mathbf{b}^s)\mathbf{g} + \boldsymbol{\tau}_r^{or}\mathbf{b}^{or}\mathbf{JL} \\
&= \boldsymbol{\tau}_r^{or}\mathbf{b}^{or}\mathbf{J}(\mathbf{g} + \mathbf{L}) \\
&= \mathbf{b}^r(\mathbf{g} + \mathbf{L}),
\end{aligned} \tag{63}$$

we can see that the difference $\mathbf{f}^{or} - \mathbf{f}_\infty^{or}$ can be considered as the projection of $\mathbf{g} + \mathbf{L}$ on the new set of vectors $\mathbf{b}^r$, where

$$\mathbf{b}^r = \mathbf{b}^{or} + \boldsymbol{\tau}_r^{or}\boldsymbol{\lambda}_{os}^{or}\mathbf{b}^s = \boldsymbol{\tau}_r^{or}\mathbf{b}^{or}\mathbf{J}. \tag{64}$$

Furthermore, from the remaining terms in the right-hand side of equation (62) we can notice that

$$\begin{aligned}
\mathbf{L} + \mathbf{a}_r\mathbf{f}_\infty^{or} + \mathbf{a}_{os}\mathbf{f}^s &= \mathbf{L} - \mathbf{a}_r\boldsymbol{\tau}_r^{or}\boldsymbol{\lambda}_{os}^{or}\mathbf{f}^s - \mathbf{a}_r\boldsymbol{\tau}_r^{or}\mathbf{b}^{or}\mathbf{JL} \\
&= (\mathbf{I} - \mathbf{a}_r\boldsymbol{\tau}_r^{or}\mathbf{b}^{or}\mathbf{J})\mathbf{L} + (\mathbf{a}_{os} - \mathbf{a}_r\boldsymbol{\tau}_r^{or}\boldsymbol{\lambda}_{os}^{or})\mathbf{f}^s \\
&= (\mathbf{I} - \mathbf{a}_r\mathbf{b}^r)\mathbf{L} + \mathbf{a}_s\mathbf{f}^s,
\end{aligned} \tag{65}$$

where

$$\mathbf{a}_s = \mathbf{a}_{os} - \mathbf{a}_r\boldsymbol{\tau}_r^{or}\boldsymbol{\lambda}_{os}^{or} = [\mathbf{I} - \mathbf{a}_r\mathbf{b}^r]\mathbf{a}_{os}. \tag{66}$$

Therefore, (62) can be cast in the form

$$\frac{\partial \mathbf{y}}{\partial t} = \mathbf{a}_r\mathbf{h}^r + \mathbf{a}_s\mathbf{h}^s, \tag{67}$$

where

$$\mathbf{h}^r = \mathbf{b}^r(\mathbf{L} + \mathbf{g}), \qquad \mathbf{h}^s = \mathbf{b}^s(\mathbf{L} + \mathbf{g}). \tag{68}$$

The derivation of (67) is the result of expanding the full right-hand side of the original equation (1) in terms of the new basis $\mathbf{a}_r$ and $\mathbf{a}_s$. The set of vectors $\mathbf{b}^r$ and $\mathbf{b}^s$ is orthogonal to the basis $\mathbf{a}_r$ and $\mathbf{a}_s$:

$$\mathbf{b}^r\mathbf{a}_r = \mathbf{I}, \quad \mathbf{b}^r\mathbf{a}_s = \mathbf{0}, \quad \mathbf{b}^s\mathbf{a}_r = \mathbf{0}, \quad \mathbf{b}^s\mathbf{a}_s = \mathbf{I}. \tag{69}$$

The usefulness of (67) is clear if we notice that

$$\mathbf{h}^r = \mathbf{f}^{or} - \mathbf{f}^{or}_{\infty}. \tag{70}$$

When $\mathbf{f}^{or}$ approaches its asymptotic value $\mathbf{f}^{or}_{\infty}$, h^r decays to an asymptotically small value. Therefore, we obtain

$$\mathbf{h}^r \approx \mathbf{0} \tag{71}$$

and the simplified system defined by (28) is recovered. In order for $\mathbf{f}^{or}$ to reach its asymptotic value, $\mathbf{f}^{or}_{\infty}$ must be a slowly varying function of time. To determine the conditions under which this is possible, we recast $\mathbf{f}^{or}_{\infty}$ using the new basis vectors as:

$$\begin{aligned} \mathbf{f}^{or}_{\infty} &= -(\mathbf{b}^r\mathbf{a}_{os})\mathbf{f}^s - \mathbf{b}^r\mathbf{L} \\ &= -(\boldsymbol{\tau}^{or}_r\boldsymbol{\lambda}^{or}_{os})\mathbf{f}^s - \mathbf{b}^r\mathbf{L}. \end{aligned} \tag{72}$$

Given that the stiffness of the original problem (1) is mainly due to the source term $\mathbf{g}$ and that $\mathbf{f}^s$ by construction varies slowly with time, it follows that the projection of the differential operator $\mathbf{L}$ on $\mathbf{b}^r$ (the fast subdspace of $\mathbf{g}$) must be negligible. In that case, $\mathbf{f}^{or}_{\infty}$ is a slowly varying function of time and (71) reduces to the algebraic relations (32).

5.3. The condition for determining M. Given the stiff reaction diffusion equation (1), the algorithm developed above produces an equivalent simplified model consisting of $N-M$ nonstiff differential equations and M algebraic relations, (35) and (36), respectively. The construction of these equations is based on the availability, at each point in time and space, of the basis vectors in $\mathbf{a}_r$ and $\mathbf{a}_s$ (and their dual in $\mathbf{b}^r$ and $\mathbf{b}^s$). These vectors can be determined either analytically or numerically. Given a basis $\mathbf{a}_{or}$ and $\mathbf{a}_{os}$ (and the dual basis $\mathbf{b}^{or}$ and $\mathbf{b}^{os}$), the CSP vectors are determined via (48), (49), (64), (66):

$$\mathbf{a}_r = \mathbf{J}\mathbf{a}_{or}\boldsymbol{\tau}^{or}_{or}, \quad \mathbf{b}^s = \mathbf{b}^{os}[\mathbf{I} - \mathbf{a}_r\mathbf{b}^{or}], \tag{73a,b}$$

$$\mathbf{b}^r = \boldsymbol{\tau}^{or}_r\mathbf{b}^{or}\mathbf{J}, \quad \mathbf{a}_s = [\mathbf{I} - \mathbf{a}_r\mathbf{b}^r]\mathbf{a}_{os}, \tag{73c,d}$$

where

$$\boldsymbol{\tau}^{or}_{or} = (\mathbf{b}^{or}\mathbf{J}\mathbf{a}_{or})^{-1}, \qquad \boldsymbol{\tau}^{or}_{or} = (\mathbf{b}^{or}\mathbf{J}\mathbf{a}_{or})^{-1}.$$

The scalar M, which denotes the number of the fast time scales and determines the partition of the basis vectors in $\mathbf{a}_r$ and $\mathbf{a}_s$, is identified as the number of the algebraic relations (30):

$$h^i = \mathbf{b}^i \cdot \mathbf{L} + B^i_1F^1 + B^i_2F^2 + \cdots + B^i_KF^K \approx 0, \quad i = 1, M, \tag{30}$$

which indicate that h^i is in some sense negligible due to significant cancellations among its additive terms. Since the amplitudes h^i are the components of the M-dimensional

vector $\mathbf{h}^r$ and since the simplified set of equations (28) is obtained by ignoring the term $\mathbf{a}_r\mathbf{h}^r$ in the original set of differential equations (25), M is determined by the number of amplitudes h^i which satisfy the condition

$$|\mathbf{a}_r\mathbf{h}^r|\Delta t_{M+1} < c_1|\mathbf{y}| + \mathbf{y}_{cut}, \tag{74a}$$

where "| |" denotes the absolute value of the elements in a vector, Δt_{M+1} is a fraction of the time scale related to the $(M+1)$th mode, c_1 is a positive number less than 1 (e.g., 10^{-2}, 10^{-3}, etc.), and $\mathbf{y}_{cut}$ is a vector whose elements are positive and much smaller in absolute value than those in $\mathbf{y}$. The two terms on the right-hand side of (74a) are related to the relative and absolute errors, respectively. Since it was assumed that the stiffness is due to the source term $\mathbf{g}$ and the term $\mathbf{b}^i \cdot \mathbf{L}$ does not contribute much in the cancellations occurring in (30), (74a) can be replaced by the condition

$$|\mathbf{a}_r\mathbf{f}^r|\Delta t_{M+1} < c_1|\mathbf{y}| + \mathbf{y}_{cut}. \tag{74b}$$

The value of Δt_{M+1} can be determined by the relation

$$\Delta t_{M+1} = \frac{c_2}{|\mathbf{b}^{M+1}\mathbf{J}\mathbf{a}_{M+1}|}, \tag{74c}$$

where c_2 is a positive number less than 1 (e.g., 1/2, 1/4, etc.). Since the denominator is an estimate of the $(M+1)$th largest eigenvalue of $\mathbf{J}$, Δt_{M+1} is a fraction of the dominant time scale due to the source term.

5.4. Remarks. Seeking the asymptotic solution of a stiff reaction-diffusion problem, the advantages of the algorithm presented in sections 4 and 5 are significant. First, it is not necessary to work with nondimensional equations and thus to identify the proper scaling for the unknowns. Furthermore, the identification of the small parameter, on the basis of which the expansion of the unknowns will be performed, is avoided. Finally, the tedious procedure of expanding the unknowns and collecting the leading order terms is not needed. As was indicated previously, when treating the problem at hand with the conventional asymptotic method in section 3, the effort of identifying the proper scaling and the small parameter as well as constructing the simplified problem requires intuition, experience, and heavy analytical work. Obviously, when the dimension of the problem under consideration is large, such an effort is impossible. On the other hand, CSP produces everything the conventional method does through an algorithm which can be used analytically or numerically and is not limited by the size or complexity of the problem at hand.

In the following, analytical results obtained with the CSP method for the chain-reaction problem (3a)–(3c) shall be presented and compared with those obtained with the conventional asymptotic method. In addition, numerical results obtained by employing the CSP method will be compared with the numerical solution of the original equation.

6. Analytical results with CSP. In section 3, the reaction-diffusion equations (3a)–(3c) were analyzed by employing conventional asymptotics. Two cases were examined, related to the different values of the reaction rate constants. In the first case, $\kappa_2 \gg \kappa_3$, two steady-state approximations were reached, while in the second case, $\kappa_2 \ll \kappa_3$, a partial equilibrium approximation was applicable. In what follows, these approximations and the corresponding simplified systems will also be derived by use of the CSP method described in sections 4 and 5. As previously mentioned, when

treating a problem with CSP there is no need to normalize the equations. However, the two different kinds of normalization introduced by (7) and (16) for the two cases treated will also be employed here for reasons of consistency and easy comparison with the results presented in section 3.

According to the CSP method, the governing equations (3a)–(3c) of the problem under consideration can be written in the vector form:

$$\frac{\partial \mathbf{y}}{\partial t} = \mathbf{a}_1 h^1 + \mathbf{a}_2 h^2 + \mathbf{a}_3 h^3, \tag{75}$$

where $\mathbf{y} = (R_1, R_2, M_1)^T$, $h^i = \mathbf{b}^i \cdot (\mathbf{L} + \mathbf{g})$, $\mathbf{a}_i$, $\mathbf{b}^i$ $(i = 1, 2, 3)$ are the CSP-provided vectors given in the Appendix, and $\mathbf{L} + \mathbf{g}$ represents the right-hand side of equations (3a)–(3c).

6.1. The steady-state approximation. First, we consider the case $\nu \to \infty$ (i.e., $\kappa_2 \gg \kappa_3$, $\omega_1 = O(\omega_2) \gg 1$). Setting $M = 2$, the CSP-provided vectors $\mathbf{a}_i$ and $\mathbf{b}^i$ $(i = 1 - 3)$ are given by the relations (A2)–(A3). The vectors $\mathbf{a}_1$, $\mathbf{a}_2$ form the $\mathbf{a}_r$ matrix, while $\mathbf{a}_3$ corresponds to $\mathbf{a}_s$. Equivalently, the $\mathbf{b}^1$, $\mathbf{b}^2$ vectors form the $\mathbf{b}^r$ matrix, while $\mathbf{b}^3$ corresponds to $\mathbf{b}^s$. On the basis of equations (27) and (28), the resulting simplified system is:

$$h^1 \approx 0, \tag{76a}$$

$$h^2 \approx 0, \tag{76b}$$

$$\frac{\partial \mathbf{y}}{\partial \tau} \approx \mathbf{a}_3 h^3. \tag{76c}$$

Taking into account the analytic expressions of $\mathbf{b}^1$, $\mathbf{b}^2$, and $\mathbf{L} + \mathbf{g}$, the expanded form of (76a)–(76b) is

$$\left(\frac{1}{1+\mu}, \frac{-\Gamma x_2}{\beta}, \frac{\Gamma}{\beta}\right) \cdot \begin{pmatrix} \alpha_1 D^2 R_1 + \kappa_1 M_1 - \kappa_2 R_1 M_1 + \kappa_3 R_2 - \kappa_4 R_1 R_2 \\ \alpha_2 D^2 R_2 + \kappa_2 R_1 M_1 - \kappa_3 R_2 - \kappa_4 R_1 R_2 \\ \alpha_3 D^2 M_1 - \kappa_1 M_1 - \kappa_2 R_1 M_1 \end{pmatrix} \approx 0, \tag{77}$$

$$\left(\frac{-B x_1}{\beta}, \frac{1}{1+\gamma}, \frac{B}{\beta}\right) \cdot \begin{pmatrix} \alpha_1 D^2 R_1 + \kappa_1 M_1 - \kappa_2 R_1 M_1 + \kappa_3 R_2 - \kappa_4 R_1 R_2 \\ \alpha_2 D^2 R_2 + \kappa_2 R_1 M_1 - \kappa_3 R_2 - \kappa_4 R_1 R_2 \\ \alpha_3 D^2 M_1 - \kappa_1 M_1 - \kappa_2 R_1 M_1 \end{pmatrix} \approx 0, \tag{78}$$

where the parameters x_1, x_2, B, Γ, β, γ, and μ are defined in the Appendix. Employing the scaling introduced by (7), (77)–(78) become

$$\left(\frac{1}{1+\hat{\mu}}, \frac{-\hat{\Gamma}\hat{x}_2}{\hat{\beta}}, \frac{\hat{\Gamma}}{\hat{\beta}}\right) \cdot \begin{pmatrix} \frac{\alpha_1}{L^2\omega_1} E^2 y_1 + \kappa_1 \left(y_3 - K y_1 y_3 + \frac{y_2}{16\nu K} - \frac{y_1 y_2}{2}\right) \\ \frac{\alpha_2}{2L^2\omega_2} E^2 y_2 + \kappa_1 \left(K y_1 y_3 - \frac{y_2}{16\nu K} - \frac{y_1 y_2}{2}\right) \\ \frac{\alpha_3}{L^2} E^2 y_3 - \kappa_1 (y_3 + K y_3) \end{pmatrix} \approx 0, \tag{79}$$

$$\left(\frac{-\hat{B}\hat{x}_1}{\hat{\beta}}, \frac{1}{1+\hat{\gamma}}, \frac{\hat{B}}{\hat{\beta}}\right) \cdot \begin{pmatrix} \frac{\alpha_1}{L^2\omega_1} E^2 y_1 + \kappa_1 K \left(\frac{y_3}{K} - y_1 y_3 + \frac{y_2}{16\nu K} - \frac{y_1 y_2}{2K}\right) \\ \frac{\alpha_2}{L^2\omega_2} E^2 y_2 + \kappa_1 K \left(y_1 y_3 - \frac{y_2}{2cK} - \frac{y_1 y_2}{2K}\right) \\ \frac{\alpha_3}{L^2} E^2 y_3 + \kappa_1 (-y_3 - K y_1 y_3) \end{pmatrix} \approx 0, \tag{80}$$

where $E = \partial/\partial z$ and the parameters $\hat{x}_1$, $\hat{x}_2$, $\hat{B}$, $\hat{\Gamma}$, $\hat{\beta}$, $\hat{\gamma}$, and $\hat{\mu}$ are also defined in the Appendix. In the limit $\nu \to \infty$ ($\kappa_1 \gg \kappa_3$) and assuming all the space derivatives to be of $O(1)$, (79)–(80) are simplified to

$$\frac{y_3}{K} - y_1 y_3 + \frac{y_2}{2cK} - \frac{y_1 y_2}{2K} \times \approx 0, \tag{81}$$

$$y_1 y_3 - \frac{y_2}{2cK} - \frac{y_1 y_2}{2K} \approx 0. \tag{82}$$

Furthermore, the system of differential equations (76c) simplifies to

$$\frac{\partial y_1}{\partial \tau} \approx \frac{1 - y_1}{2y_3}(q_1 E^2 y_3 - 3y_3), \tag{83a}$$

$$\frac{\partial y_2}{\partial \tau} \approx \frac{y_3 - y_2 + y_1 y_2}{y_1 y_3}(q_2 E^2 y_3 - 3y_3), \tag{83b}$$

$$\frac{\partial y_3}{\partial \tau} \approx (q_3 E^2 y_3 - 3y_3). \tag{83c}$$

Equations (83a)–(83c) govern the evolution of the trajectory on the manifold defined by (81)–(82). Obviously, equations (81) and (82) are identical to equations (13a)–(13b) obtained through conventional asymptotics and provide the same solutions, i.e., (14a)–(14b):

$$y_1 \approx 1, \tag{84}$$

$$y_2 \approx y_3, \tag{85}$$

which are the steady-stage relations for y_1 and y_2.

The simplified system of equations might consist either of the three differential equations (83a)–(83c) or of the two algebraic relations (81), (82) and one of the differential equations (83a)–(83c). In order to determine which two of the three differential equations (83a)–(83c) can be substituted by the two algebraic relations (84)–(85), the CSP pointer is employed. We obtain

$$\operatorname{diag}(\mathbf{a}_r \mathbf{b}^r) = \operatorname{diag}(\mathbf{a}_1 \mathbf{b}^1 + \mathbf{a}_2 \mathbf{b}^2) = \left(\frac{1}{1+\hat{\mu}}, \frac{1}{1+\hat{\gamma}}, \frac{\hat{x}_1 \hat{\Gamma} + \hat{x}_2 \hat{B}}{\hat{\beta}} \right), \tag{86a}$$

which in the $\nu \to \infty$ limit becomes

$$\operatorname{diag}(\mathbf{a}_r \mathbf{b}^r) = \operatorname{diag}(\mathbf{a}_1 \mathbf{b}^1 + \mathbf{a}_2 \mathbf{b}^2) = (1, 1, 0). \tag{86b}$$

This suggests that the two unknowns y_1 and y_2 can be determined by the algebraic relations (84)–(85) while y_3 will be determined by the differential equation (83c).

6.2. The partial equilibrium approximation. We consider now the case $\nu \to 0$ ($\kappa_2 \ll \kappa_3, \omega_1 = O(\omega_2) \gg 1$). Setting $M = 1$, the CSP provided vectors $\mathbf{a}_i$ and $\mathbf{b}^i$ ($i = 1, 3$) are given by equations (A6)–(A7). The $\mathbf{a}_r$, $\mathbf{b}^r$ vectors are formed by $\mathbf{a}_1$ and $\mathbf{b}^1$, respectively, while $\mathbf{a}_s$, $\mathbf{b}^s$ are composed by $\mathbf{a}_2$, $\mathbf{a}_3$ and $\mathbf{b}^2$, $\mathbf{b}^3$, respectively. The simplified system obtained is

$$h^1 \approx 0, \tag{87a}$$

$$\frac{\partial \mathbf{y}}{\partial t} \approx \mathbf{a}_2 h^2 + \mathbf{a}_3 h^3. \tag{87b}$$

Using the expressions of $\mathbf{b}^1$ and $\mathbf{L}+\mathbf{g}$, the analytic form of (87a) is

$$(z_1, z_2, z_3) \cdot \begin{pmatrix} \alpha_1 D^2 R_1 + \kappa_1 M_1 - \kappa_1 R_1 M_1 + \kappa_3 R_2 - \kappa_4 R_1 R_2 \\ \alpha_2 D^2 R_2 + \kappa_2 R_1 M_1 - \kappa_3 R_2 - \kappa_4 R_1 R_2 \\ \alpha_3 D^2 M_1 - \kappa_1 M_1 - \kappa_2 R_1 M_1 \end{pmatrix} \approx 0, \tag{88}$$

where the parameters z_1, z_2, and z_3 are defined in the Appendix. Introducing the normalization defined by equations (16), (18), the above relation becomes

$$(\hat{z}_1, \hat{z}_2, \hat{z}_3) \cdot \begin{pmatrix} \dfrac{\alpha_1}{L^2\sqrt{\omega_1}} E^2 y_1 + \dfrac{y_3}{\sqrt{\kappa_2}} - \dfrac{1}{\sqrt{\kappa_1}}(y_1 y_3 - y_2) - \dfrac{8\nu\sqrt{\omega_1}}{\sqrt{\kappa_1}} y_1 y_2 \\ \dfrac{8\nu\alpha_2}{\chi L^2} E^2 y_2 + \dfrac{1}{\sqrt{\kappa_1}}(y_1 y_3 - y_2) - \dfrac{8\nu\kappa_2}{\chi} y_1 y_2 \\ \dfrac{\alpha_3 \chi}{L^2} E^2 y_3 - \dfrac{y_3}{\sqrt{\kappa_2}} - \dfrac{y_1 y_3}{\sqrt{\kappa_1}} \end{pmatrix} \approx 0, \tag{89}$$

where $E = \partial/\partial z$ and $\hat{z}_1$, $\hat{z}_2$, $\hat{z}_3$ are also defined in the Appendix. In the limit $\nu \to 0$ and assuming the space derivatives are of $O(1)$, (89) simplifies to

$$y_1 y_3 - y_2 \approx 0, \tag{90}$$

which is indentical to (19) expressing the partial equilibrium approximation for the two propagating reactions (2a)–(2c). Using the expressions (A6), (A7) for $\boldsymbol{\alpha}_2, h^2, \boldsymbol{\alpha}_3, h^3$, the simplified system of differential equations (87b) is analytically written as

$$\begin{aligned} \frac{\partial}{\partial t}\begin{pmatrix} R_1 \\ R_2 \\ M_1 \end{pmatrix} &= \begin{pmatrix} -z_2 \\ 1 - x_1 z_2 \\ -x_2 z_2 \end{pmatrix} (-x_1, 1, 0) \cdot \begin{pmatrix} (L+g)_1 \\ (L+g)_2 \\ (L+g)_3 \end{pmatrix} \\ &\quad + \begin{pmatrix} -z_3 \\ 1 - x_1 z_3 \\ 1 - x_2 z_3 \end{pmatrix} (-x_2, 0, 1) \cdot \begin{pmatrix} (L+g)_1 \\ (L+g)_2 \\ (L+g)_3 \end{pmatrix}, \end{aligned} \tag{91}$$

where $(L+g)_i$ is the ith component of the vector $\mathbf{L}+\mathbf{g}$. Employing the scaling introduced via (16) and considering the limit $\nu \to 0$, the system of differential equations (91) simplifies to

$$\frac{\partial y_1}{\partial \tau} \approx p_1 E^2 y_1 + \chi y_3, \tag{92a}$$

$$\frac{\partial y_2}{\partial \tau} \approx y_3 p_1 E^2 y_1 + y_1 p_3 E^2 y_3 + \chi y_3^2 - y_1^2 y_3, \tag{92b}$$

$$\frac{\partial y_3}{\partial \tau} \approx p_3 E^2 y_3 - y_1 y_3, \tag{92c}$$

which is identical to equations (21a)–(21c) obtained by the conventional method. The simplified system consists either of the three differential equations (92a)–(92c) or of the algebraic relation (90) and two of the equations (92a)–(92c). In order to determine which one of the three differential equations (91a)–(91c) can be replaced by the algebraic relation (90), the CSP pointer is employed providing:

$$\mathrm{diag}(\mathbf{a}_r \mathbf{b}^r) = \mathrm{diag}(\mathbf{a}_1 \mathbf{b}^1) = (\hat{z}_1, \hat{x}_1 \hat{z}_2, \hat{x}_2 \hat{z}_3). \tag{93a}$$

In the $\nu \to 0$ limit the pointer reduces to

$$\mathrm{diag}(\mathbf{a}_r \mathbf{b}^r) = \mathrm{diag}(\mathbf{a}_1 \mathbf{b}^1) = (0, 1, 0). \tag{93b}$$

This suggests that the unknown y_2 can be determined from the algebraic relation (90) while y_1 and y_3 will be determined by the differential equations (92a) and (92c), respectively.

6.3. Remarks. In section 6.1 it was shown that in the case where $M = 2$, CSP provided identical algebraic relations to the ones obtained by the conventional asymptotic method using the steady-state approximation for y_1 and y_2. In addition, CSP provided the asymptotic system of differential equations (83a)–(83c) and the correct structure of the simplified system, i.e., equations (81), (82), and (83c). In section 6.2 for the case $M = 1$, it was shown that the simplified system provided by CSP is identical to the one obtained by the conventional asymptotic method using the partial equilibrium approximation. In both cases, apart from the derivation of the simplified system, all the related physical information was provided by CSP data without making use of any scaling or imposing any assumption, as was needed when the conventional asymptotic method was employed. Note that in obtaining the analytical results presented in sections 6.1 and 6.2, only the value of M had to be specified. However, as was discussed in section 5.3, in the numerical implementation of the method the value of M is automatically computed.

At this point, it is significant to emphasize the importance of the CSP pointer in the selection of the M components of $\mathbf{y}$ that can be solved from the algebraic relations (36). Note that this selection determines the remaining $N-M$ components of $\mathbf{y}$ which will be computed by the corresponding components of the differential equations (35). In order to demonstrate the importance of the pointer, consider the case $\nu \to \infty$ (treated in section 6.1) and the solution (85) of the algebraic relation (82); (81)–(82) were assigned by the pointer for the computation of R_1 and R_2. In dimensional form and in the limit $\nu \to \infty$, (85) becomes

$$R_2 = \frac{1}{\omega_2} M_1. \tag{94}$$

Since in the example analyzed here it was assumed that $\omega_2 \gg 1$, it is clear that a perturbation in M_1 will produce a small response in R_2. On the other hand, if M_1 was chosen to be computed from (94), a perturbation in R_2 will result in a large response in M_1. Therefore, it is seen that the CSP pointer chooses the components of $\mathbf{y}$ which produce the most stable solution from the algebraic relations (36).

7. Computational aspects. The advantages of the CSP method for the numerical simulation of physical phenomena governed by the transient reaction-diffusion equation (1) can be demonstrated in simple terms as follows. Consider the case where the ith element of the spatial differential operator $\mathbf{L}$ is the Laplacian operator ∇^2 acting on y^i multiplied by a constant q^i. Equation (1) then becomes

$$\frac{\partial y^i}{\partial t} = q^i \nabla^2 y^i + g^i(\mathbf{y}), \tag{95}$$

where y^i and g^i are the ith components of $\mathbf{y}$ and $\mathbf{g}$, respectively. Given that $\mathbf{g}$ introduces stiffness, (95) can be solved with an implicit scheme for stability reasons [15, 16, 17] or by blended multistep methods, which are characterized by a large stability region [18]. However, due to the numerical solution of the resulting system of algebraic equations at each time step, these schemes can be slow and, therefore, not suitable. The use of an explicit scheme (which is simple, accurate on the fast time scales [15], and requires no additional operations at each time step) is hindered by the

small time step imposed by stability considerations. This problem can be faced with CSP as follows. For simplicity, let us employ the forward-in-time, centered-in-space (FTCS) scheme [19, 20]. In that case, the discretized form of (95) is

$$y_j^{i,n+1} = y_j^{i,n} + p^i D^2 y_j^{i,n} + \Delta t g_j^{i,n}, \tag{96a}$$

where

$$D^2 y_j^{i,n} = [y_{j+1}^{i,n} - 2y_j^{i,n} + y_{j-1}^{i,n}] \tag{96b}$$

and $p^i = q^i \Delta t / \Delta x^2$, Δt is the time step, Δx is the spacing between the grids and "n" and "j" characterize the step in time and space, respectively. For stability [19, 20], the time step must either satisfy the condition

$$\Delta t \leq \frac{\Delta x^2}{2 \max(q^i)} \tag{96c}$$

or be of the order of the reciprocal of the largest eigenvalue of $\mathbf{g}$, whichever is smaller. In other words, the size of the time step is determined by the stiffness of the spatial operator or of the source term (depending on which stiffness is more severe).

For the reaction-diffusion problem considered here, it was assumed that the stiffness is mainly due to the source term $\mathbf{g}$. In that case, the simplified system of differential equations (28), which is free of temporal stiffness, allows the use of a time step which respects the stiffness of the spatial operator only (see the comments on (72) in section 5.2). Applying the FTCS scheme, the discretized form of (28) is

$$y_j^{i,n+1} = y_j^{i,n} + \sum_{s=M+1}^{N} a_s^{i,n} \left[p^i \sum_{k=1}^{N} b_k^{s,n} D y_j^{k,n} + \Delta t \sum_{k=1}^{N} b_k^{s,n} g_j^{k,n} \right]. \tag{97}$$

As was discussed in section 4, there are two options for the replacement of the full discretized equation (96a) by the simplified equation (97). First, the full equation (96a) can be directly replaced by the simplified equation (97). In that case, the use of the "homogeneous correction" must be explored. According to this correction [10, 11], at the nth time level and each spatial node the components of $\mathbf{y}$ must be reevaluated as

$$\tilde{\mathbf{y}}_j^n = \mathbf{y}_j^n - (\mathbf{a}_r \boldsymbol{\tau}_r^r \mathbf{f}^r)_j^n (\mathbf{y}_j^n) \tag{98}$$

and then proceed to the $(n+1)$th level by substituting $\tilde{\mathbf{y}}_j^n$ instead of $\mathbf{y}_j^n$ in the right-hand side of (97). As was indicated in (33), this correction accounts for the fast time scales and guarantees that the algebraic relations (36), which were used for the simplification of (96a), are to leading order satisfied. An alternative procedure consists of solving the algebraic relations (36) for the M unknowns indicated by the CSP pointer (as was shown in section 6) and the appropriate components of (97) for the remaining $N - M$ unknowns.

The fact that spatial stiffness occurs in a limited region of the spatial computational domain must be explored. It was shown in section 5.2 that in order to simplify the original equation (1) and obtain an approximate solution using the discretized equation (97), the differential operator $\mathbf{L}$ must be less stiff than the source term $\mathbf{g}$. In addition, it was shown that the algorithm proposed here reduces the stiffness of the source term down to the stiffness of the spatial operator (i.e., (72)). Since at any point

in time, different degrees of stiffness of the differential operator can be encountered across the spatial domain, it follows that different degrees of simplified problems (in the form of (97)) can be constructed. As a result, different time steps will be allowed at different grid points. The options here are either to use the smallest time step to advance to the next time level or to use different time steps at different grid points (very much suited if only the steady state is sought [15]). In addition, since the degree of the allowed simplification is directly related to the stiffness of the spatial operator, a simple measure for the construction of an optimum nonuniform spatial grid is provided.

The purpose of this manuscript is not to address all these issues but rather to present the theoretical background of the proposed algorithm and to provide preliminary results of its usefulness and its accuracy. In section 6 such results were presented from the analytic implementation of the method. Next, similar results will be presented from its numerical use.

8. Numerical results with CSP. Consider the reaction-diffusion problem (3a)–(3c) along with the boundary conditions (6a)–(6b). All the diffusion coefficients are taken equal to 1 (i.e., $\alpha_1 = \alpha_2 = \alpha_3 = 1$) and the reaction rate constants are defined as $\kappa_1 = 1, \kappa_2 = 10^3, \kappa_3 = 1$, and $\kappa_4 = 10^6$. This set of parameters yields $\nu = 125$, which refers to the $\nu \to \infty$ case treated analytically in sections 3.1 and 6.1. Substituting the scaling (7) in (14a)–(14b) and using the values for the rate constants as specified above, it can be shown that the following asymptotic relations hold:

$$R_1 \approx 0.5E - 3, \qquad R_2 \approx 1.0E - 3M_1. \tag{99}$$

In the following, we consider the case where the solution has reached steady state. In all computations to be reported next, the steady state form of (3a)–(3c) was discretized on a uniform grid with $\Delta x = 0.02$ (50 grid points) using centered differences. The resulting system of nonlinear algebraic equations was solved with the Newton method.

8.1. Diagnostics. The numerical solution of the original system of differential equations (3a)–(3c) satisfying the boundary conditions (6a)–(6b) is presented in Fig. 1. It is shown that in the region next to the left boundary, the unknowns R_1 and R_2 undergo a rapid change, exhibiting a boundary layer behavior. Away from that region and throughout the remaining domain they attain their asymptotic values specified by (99). The existence of a region where the unknowns exhibit a rapid evolution is a manifestation of spatial stiffness.

In order to examine the stiffness introduced by the source term $\mathbf{g}$, the eigenvalues of its Jacobian were calculated throughout the computational domain. Fig. 2 displays the ratio of successive (in magnitude) eigenvalues as a function of x. It is shown that, while the first two eigenvalues are of the same order, a significant gap exists between the second and third eigenvalues. As was indicated in section 5, it is exactly this gap which causes the stiffness due to the source term. The ratio of these two eigenvalues is a measure of the stiffness due to $\mathbf{g}$. Since the large gap occurs between the second and third eigenvalues, the results of Fig. 2 indicate that counting the stiffness due to $\mathbf{g}$ alone, there must be two fast time scales producing two algebraic relations in the form of (32).

In order to verify the statement above, the three amplitudes f^1, f^2, and f^3,

$$f^i = B_1^i F^1 + B_2^i F^2 + B_3^i F^3 + B_4^i F^4, \tag{100}$$

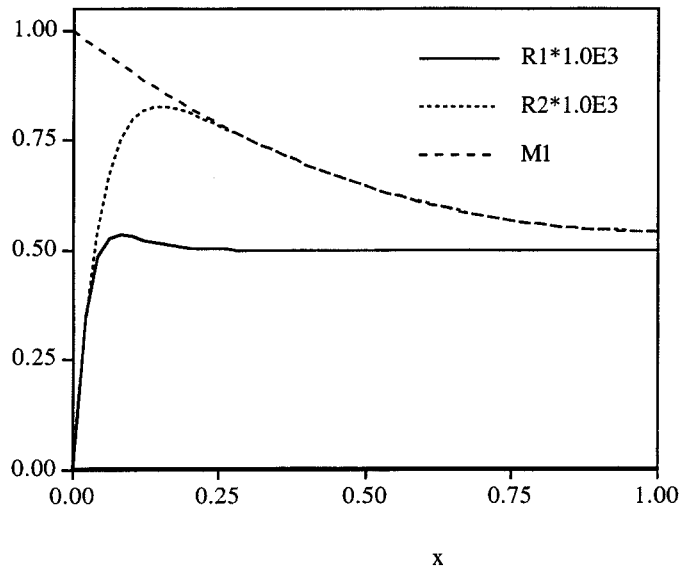

FIG. 1. *The solution of the original equations* (3a)–(3c) *and* (6a)–(6b).

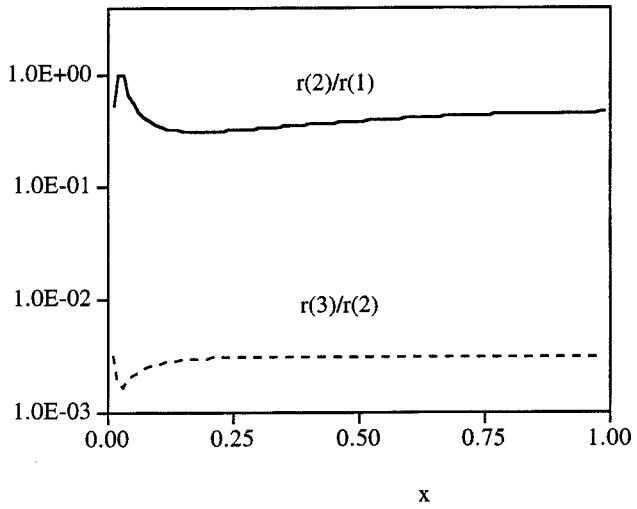

FIG. 2. *The eigenvalue ratios. r(i); i*th *eigenvalue.*

were calculated and are presented in Fig. 3a as a function of x. It is shown that starting from the left boundary, where spatial stiffness occurs, the first two amplitudes decrease close to an exponential rate. Outside the boundary layer region they retain their small asymptotic value. The third amplitude stays throughout the domain $O(1)$. With the purpose of detecting possible cancellations among the four additive terms in the expressions for the three amplitudes, the following ratios were calculated:

$$\frac{f^i}{\text{norm}(f^i)} = \frac{B_1^i F^1 + B_2^i F^2 + B_3^i F^3 + B_4^i F^4}{|B_1^i F^1| + |B_2^i F^2| + |B_3^i F^3| + |B_4^i F^4|}. \tag{101}$$

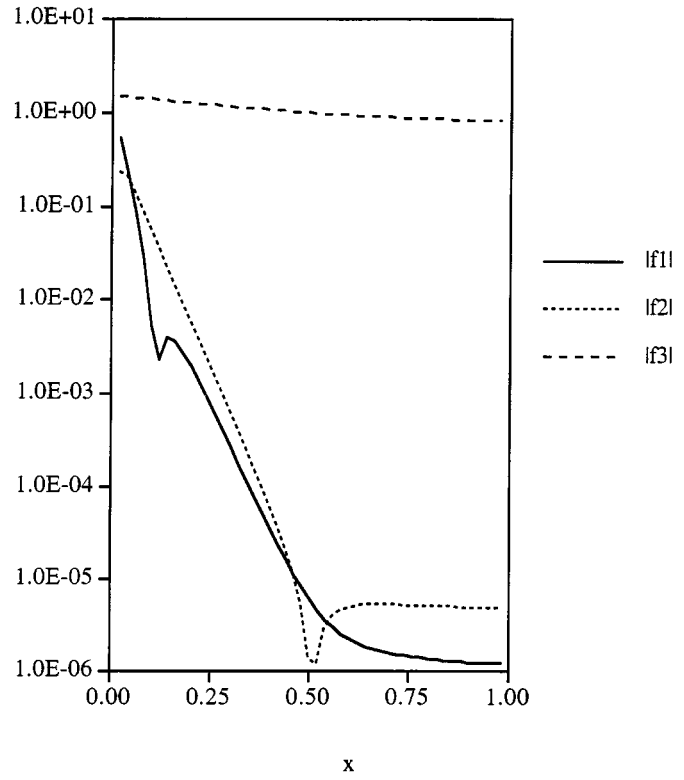

FIG. 3a. *The amplitudes f^1, f^2, and f^3; equation* (100).

It is evident that small values of this ratio indicate large cancellations in (100). The results displayed in Fig. 3b show that the small asymptotic values attained by f^1 and f^2 away from the left boundary are indeed the result of significant cancellations. In addition, it is shown that no cancellations occur in the expression for f^3.

Finally, in order to examine the significance of the contribution of the spatial operator $\mathbf{L}$ in the relations (71), the product $\mathbf{b}^i \cdot \mathbf{L}$ was computed throughout the computational domain. The distribution of the ratio

$$\frac{\mathbf{b}^i \cdot \mathbf{L}}{\text{norm}(h^i)} = \frac{\mathbf{b}^i \cdot \mathbf{L}}{|\mathbf{b}^i \cdot \mathbf{L}| + |B_1^i F^1| + |B_2^i F^2| + |B_3^i F^3| + |B_4^i F^4|}, \tag{102}$$

shown in Fig. 4, indicates that $\mathbf{b}^1 \cdot \mathbf{L}$ and $\mathbf{b}^2 \cdot \mathbf{L}$ are significant additive terms in the expressions for h^1 and h^2 (see (30)), only in the region close to the left boundary where a boundary layer exists. Away from this region, the two projections of the spatial operator are insignificant relative to the remaining algebraic terms. On the other hand, it is shown that $\mathbf{b}^3 \cdot \mathbf{L}$ is always important in the expression for h^3.

8.2. Accuracy of the simplified system. A code was developed for the solution of the steady-state reaction-diffusion problem (1) on the basis of the CSP theory presented here. The structure of the code is as follows. Given a solution $\mathbf{y}_j^n$ (where the subscript "j" refers to the grid point and the superscript "n" refers to the nth iteration level), the vectors $\mathbf{a}_r$, $\mathbf{a}_s$, $\mathbf{b}^r$, and $\mathbf{b}^s$ are computed using the formulas (73a)–(73d). The initial set of vectors $\mathbf{a} = [\mathbf{a}_{or}\mathbf{a}_{os}]$ and $\mathbf{b} = [\mathbf{b}^{or}\mathbf{b}^{os}]^T$ is set equal to the

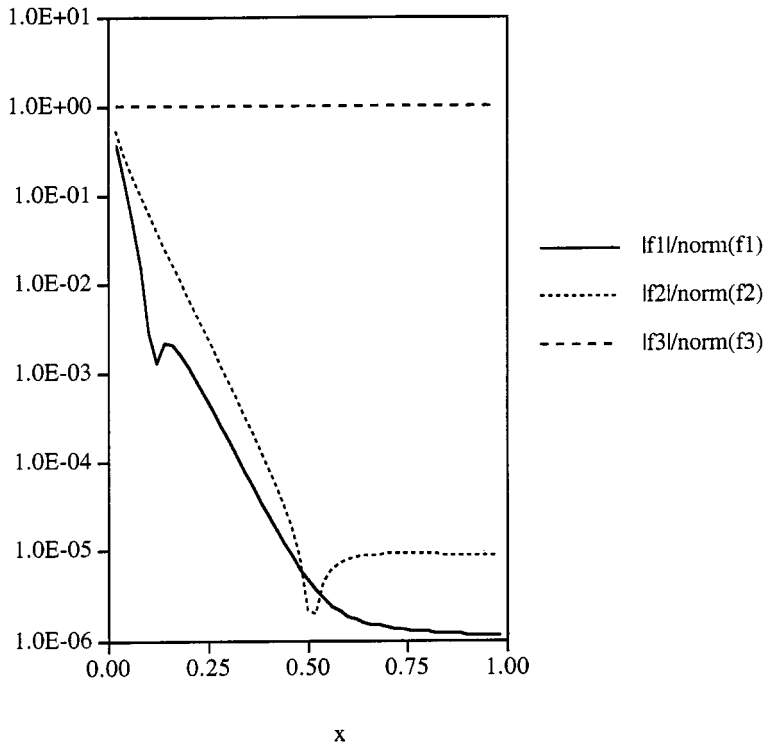

FIG. 3b. *The cancellations in the expressions for the amplitudes f^1, f^2, and f^3; equation* (101).

unit matrix as stated in (A1) of the Appendix. The computation of the set of basis vectors is performed along each point in time and at each grid point using (74b) with $c_2 = 0.25$ and $\mathbf{y}_{cut} = \mathbf{0}$.

As was discussed in section 5.3, the value of M is determined as follows. First, M is set equal to 1 and the basis vectors and the amplitude f^1 are computed. If the following relation is found to be valid,

$$|\mathbf{a}_1 f^1|\Delta t_2 \leq c_1|\mathbf{y}_j^n|, \tag{103a}$$

then the amplitude f^1 is declared exhausted. Subsequently, M is set equal to 2, the basis vectors and the amplitudes f^1 and f^2 are computed, and the validity of the following relation is tested:

$$|\mathbf{a}_1 f^1 + \mathbf{a}_2 f^2|\Delta t_3 \leq c_1|\mathbf{y}_j^n|. \tag{103b}$$

If this relation is valid, the two amplitudes f^1 and f^2 are declared exhausted. M keeps increasing by 1 and the process described previously is repeated up to the value of M for which the inequality

$$|\mathbf{a}_1 f^1 + \mathbf{a}_2 f^2 + \cdots + \mathbf{a}_M f^M|\Delta t_{M+1} \leq c_1|\mathbf{y}_j^n| \tag{103c}$$

is valid. Having determined M as the number of the exhausted amplitudes, the M components of $\mathbf{y}$, which are computed from the algebraic relations (36), are identified by the CSP pointer. The remaining $N - M$ unknowns determine the components in

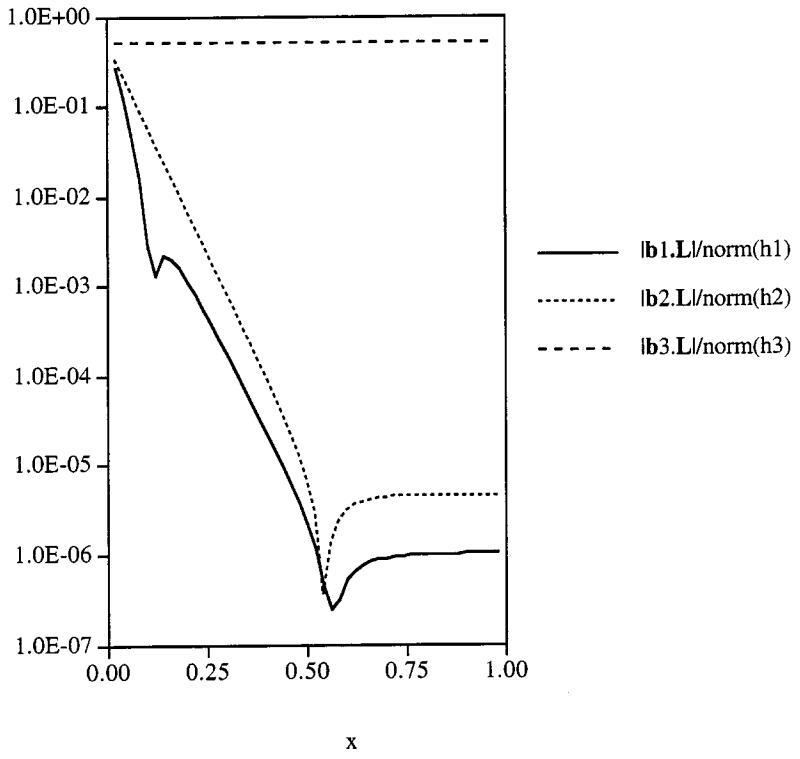

FIG. 4. *The relative importance of* $\mathbf{b}^i \cdot \mathbf{L}$ *in the expression* h^i*; equation* (102).

(35) that are eventually discretized. The process described is repeated at each grid point. The boundary conditions are handled in their original form. The resulting system of nonlinear algebraic equations is solved with the Newton method.

Numerical results were obtained with $c_1 = 1.0E{-}3$ and $c_1 = 1.0E{-}2$. The relative error (r.e.) of the solution of the simplified problem with respect to the solution of the original problem (3a)–(3c), (6a), (6b), i.e.,

$$\text{r.e.}(y^i) = \left| 1 - \frac{y^i_{\text{simpl.}}}{y^i_{\text{original}}} \right|,$$

and the corresponding distribution of M are displayed in Figs. 5a, 5b and 6a, 6b. Both Figs. 5a and 6a show that the error stays within the bounds specified by c_1. For the $c_1 = 1.0E-3$ case, Fig. 5b shows that in the region $0 \le x \le 0.14$ where $M = 0$, the full equations were discretized. From $x = 0.16$ (where approximately the first boundary layer ends) and up to $x = 0.24$ (outside of where the second boundary layer ends), $M = 1$ and the algorithm switches to the simplified problem consisting of one algebraic relation (set by the CSP pointer to be solved for R_1) and two differential equations:

$$f_1 = 0, \tag{104a}$$

$$\binom{a_{2,2}}{a_{2,3}} \mathbf{b}_2 \cdot (\mathbf{L} + \mathbf{g}) + \binom{a_{3,2}}{a_{3,3}} \mathbf{b}_3 \cdot (\mathbf{L} + \mathbf{g}) = 0, \tag{104b}$$

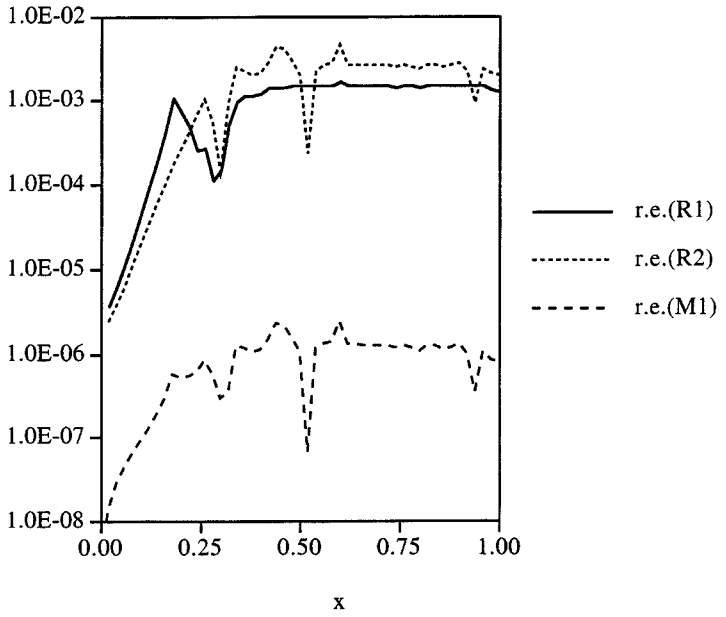

FIG. 5a. *The relative error of the numerical solution to the simplified problem;* $c = 1.0E-3$.

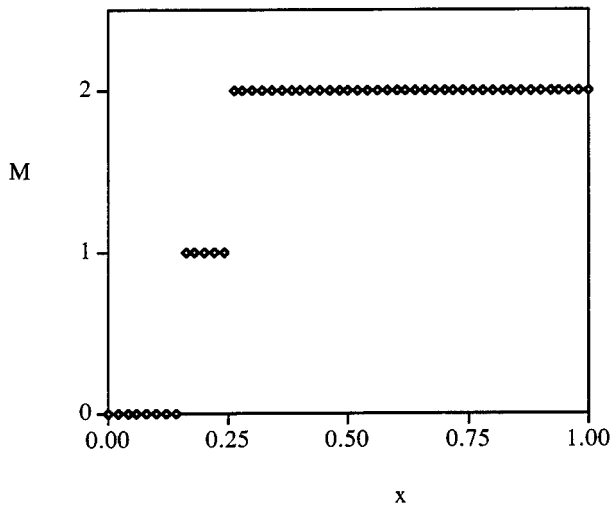

FIG. 5b. *The distribution of* M; $c = 1.0E-3$.

where $a_{i,j}$ is the jth element of $\mathbf{a}_i$. Finally, in the region $0.26 \leq x \leq 1.0$ (outside of both boundary layers), $M = 2$ and the algorithm considers the simplified problem consisting of two algebraic relations (set by the CSP pointer to be solved for R_1 and R_2) and one differential equation:

$$f_1 = 0, \tag{105a}$$

$$f_2 = 0, \tag{105b}$$

$$a_{3,3}\mathbf{b}_3 \cdot (\mathbf{L} + \mathbf{g}) = 0. \tag{105c}$$

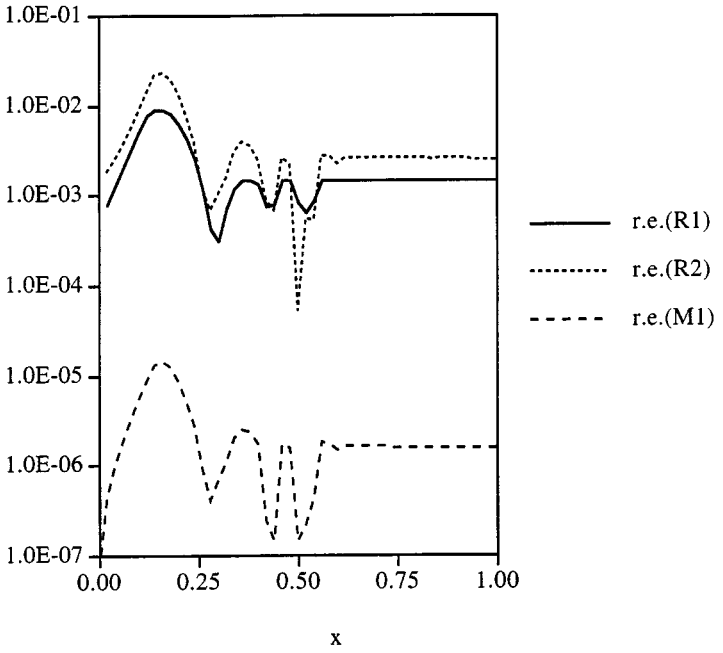

FIG. 6a. *The relative error of the numerical solution to the simplified problem;* $c = 1.0E - 2$.

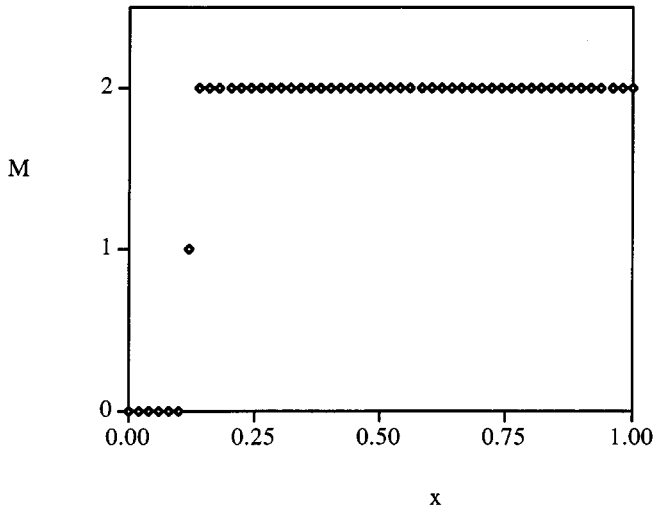

FIG. 6b. *The distribution of* M; $c = 1.0E - 2$.

Similar conclusions can be drawn from Fig. 6b for the $c_1 = 1.0E - 2$ case. Since the accuracy requirement is now less stringent, the algorithm switches to the $M = 1$ and $M = 2$ simplified problems closer to the left boundary (where a boundary layer exists) than in the case where $c_1 = 1.0E - 3$.

9. Conclusions. The CSP method was applied for the simplification of a stiff reaction-diffusion problem of the form of (1), in the case where the stiffness is mainly

due to the source term. The conventional way of treating these problems is to resort either to asymptotic methods or to implicit numerical schemes. Use of asymptotic methods is a troublesome procedure since heavy analytical work is required and also a priori estimates and theoretical assumptions must be imposed. On the other hand, implicit schemes might be difficult to employ due to the large nonlinear systems that must be solved on each time step.

In sections 4 and 5 it was shown that the CSP method can provide a simplified nonstiff system of equations which can replace the original one. Its form evolves with time and space and its accuracy increases with stiffness. Since the CSP method is completely programmable, the simplified system can be obtained either analytically or numerically. Specifically, it was shown that the original N differential equations can be replaced by $(N-M)$ nonstiff differential equations and M algebraic equations. The regions where such a simplified system can be constructed by CSP as well as the value of M, depend on the strength of the temporal stiffness in comparison to the spatial stiffness. If temporal stiffness dominates, simplified systems can be constructed which are free of the stiffness in excess of the spatial one. On the other hand, if the spatial stiffness is the dominant one, no simplification is possible. Use of the simplified system reduces the temporal stiffness so that explicit schemes and large time steps can be employed. The overall efficiency of the proposed algorithm depends on the outcome of the speedup due to the use of explicit schemes (and large time steps) and the slowdown due to the additional operations for the computation of the basis vectors. The latter issue is not expected to be significant since the Jacobian $\mathbf{J}$ in (73a)–(73d) for the basis vectors can always be provided in analytic form.

For the specific reaction-diffusion equation (3a)–(3c) considered here, the CSP method was employed in section 6 analytically for two limiting sets of reaction rate constants providing the same results with those obtained by the conventional asymptotic methods. In both cases, the algebraic relations (77)–(78) and (88), respectively, were obtained by a simple algorithm without having to define the correct scaling, take the appropriate limit, or impose any assumptions. The same comment is valid for the derivation of the simplified set of differential equations ((83a)–(83c) and (91), respectively). Furthermore, the correct set of algebraic and differential equations making up the simplified model was obtained by simply employing the CSP pointer.

The full numerical implementation of the CSP method for the solution of stiff PDEs requires the examination of several alternatives for the algorithm's optimum performance. All these alternatives were stated in section 7. The numerical results presented in section 8 validate all the theoretical aspects of the method (such as the decay of the fast amplitudes f^r due to cancellations among their additive terms, the insignificance of the product $\mathbf{b}^r \cdot \mathbf{L}$ outside the regions in which spatial stiffness occurs, etc.). In addition, it was demonstrated that, depending on the spatial stiffness, different levels of simplifications are possible. Finally, the accuracy of the method was shown to be in accordance with the theoretical expectations.

Appendix. The basis vectors for the $M = 2$ and $M = 1$ cases. The CSP vectors are obtained from the formulas (73a)–(73d). For the constant set of vectors in $\mathbf{a}_o = [\mathbf{a}_{or}, \mathbf{a}_{os}]$ and $\mathbf{b}^o = [\mathbf{b}^{or}, \mathbf{b}^{os}]^T$, the following choice was made:

$$\mathbf{a}_o = \mathbf{b}^o = \begin{bmatrix} 1 & 0 & 0 \\ 0 & 1 & 0 \\ 0 & 0 & 1 \end{bmatrix}. \tag{A1}$$

Setting $M = 2$, (73a)–(73d) provide the following basis vectors:

$$\mathbf{a}_r = \begin{bmatrix} 1 & 0 \\ 0 & 1 \\ x_1 & x_2 \end{bmatrix}, \qquad \mathbf{a}_s = \frac{1}{\beta} \begin{bmatrix} -\Gamma \\ -B \\ \beta - \Gamma x_1 - B x_2 \end{bmatrix}, \tag{A2}$$

$$\mathbf{b}^r = \begin{bmatrix} \dfrac{1}{1+\mu} & \dfrac{-\Gamma x_2}{\beta} & \dfrac{\Gamma}{\beta} \\ \dfrac{-B x_1}{\beta} & \dfrac{1}{1+\gamma} & \dfrac{B}{\beta} \end{bmatrix}, \qquad \mathbf{b}^s = [-x_1 \quad -x_2 \quad 1], \tag{A3}$$

where

$$\beta = A + B x_2 + \Gamma x_1, \quad \gamma = \left(\frac{B x_2}{A + \Gamma x_1} \right), \quad \mu = \left(\frac{\Gamma x_1}{A + B x_2} \right),$$

$$x_1 = \frac{k_2 M_1 (k_3 + k_4 R_1)}{2k_4 (k_3 R_2 + k_2 R_1 M_1)}, \quad x_2 = \frac{k_2 M_1 (k_3 - k_4 R_1)}{2k_4 (k_3 R_2 + k_2 R_1 M_1)},$$

$$A = 2k_4 (k_3 R_2 + k_2 R_1 M_1), \quad B = -k_1 (k_2 M_1 - k_4 R_2) - 2k_2 k_4 R_1 R_2,$$

$$\Gamma = -k_1 k_3 - k_1 k_4 R_1 + 2k_2 k_4 R_1 R_1.$$

Employing the scaling introduced via (7)–(8) to the CSP vectors given by (A2)–(A3), the scaled basis vectors $\hat{\boldsymbol{\alpha}}_r, \hat{\boldsymbol{\alpha}}_s, \hat{\mathbf{b}}_r, \hat{\mathbf{b}}_s$ are given as follows:

$$\hat{\boldsymbol{\alpha}}_r = \begin{bmatrix} 1 & 0 \\ 0 & 1 \\ \hat{x}_1 & \hat{x}_2 \end{bmatrix}, \qquad \hat{\boldsymbol{\alpha}}_s = \frac{1}{\hat{\beta}} \begin{bmatrix} -\hat{\Gamma} \\ -\hat{B} \\ \hat{\beta} - \hat{\Gamma} \hat{x}_1 - \hat{B} \hat{x}_2 \end{bmatrix}, \tag{A4}$$

$$\hat{\mathbf{b}}^r = \begin{bmatrix} \dfrac{1}{1+\hat{\mu}} & \dfrac{-\hat{\Gamma} \hat{x}_2}{\hat{\beta}} & \dfrac{\hat{\Gamma}}{\hat{\beta}} \\ \dfrac{-\hat{B} \hat{x}_1}{\hat{\beta}} & \dfrac{1}{1+\hat{\gamma}} & \dfrac{\hat{B}}{\hat{\beta}} \end{bmatrix}, \qquad \hat{\mathbf{b}}^s = [-\hat{x}_1 \quad -\hat{x}_2 \quad 1], \tag{A5}$$

where:

$$\hat{x}_1 = \frac{y_3 + 8\nu K y_1 y_3}{\dfrac{y_2}{K} + 16\nu K y_1 y_3}, \qquad \hat{x}_2 = \frac{y_3 - 8\nu K y_1 y_3}{\dfrac{y_2}{K} + 16\nu K y_1 y_3},$$

$$\hat{\beta} = \hat{A} + \hat{B} \hat{x}_2 + \hat{\Gamma} \hat{x}_1, \quad \hat{\gamma} = \frac{\hat{B} \hat{x}_2}{\hat{A} + \hat{\Gamma} \hat{x}_1}, \quad \hat{\mu} = \frac{\hat{\Gamma} \hat{x}_1}{\hat{A} + \hat{B} \hat{x}_2},$$

$$\hat{A} = \kappa_2 \kappa_3 \left(\frac{y_2}{K} + 16\nu K y_1 y_3 \right),$$

$$\hat{B} = -\kappa_1 \kappa_2 \left(y_3 - \frac{y_2}{2K} + y_1 y_2 \right),$$

$$\hat{\Gamma} = -\kappa_1 \kappa_3 (1 + 8\nu K - 16\nu K^2 y_1^2).$$

Setting $M = 1$, (73a)–(73d) yield

$$\mathbf{a}_r = \begin{bmatrix} 1 \\ x_1 \\ x_2 \end{bmatrix}, \qquad \mathbf{a}_s = \begin{bmatrix} -z_2 & -z_3 \\ 1 - x_1 z_2 & -x_1 z_3 \\ -x_2 z_2 & 1 - x_2 z_3 \end{bmatrix}, \tag{A6}$$

$$\mathbf{b}^r = [z_1 \quad z_2 \quad z_3], \qquad \mathbf{b}^s = \begin{bmatrix} -x_1 & 1 & 0 \\ -x_2 & 0 & 1 \end{bmatrix}, \tag{A7}$$

where

$$\begin{aligned} x_1 &= \frac{-(k_2 M_1 - k_4 R_2)}{k_2 M_1 + k_4 R_2}, \qquad x_2 = \frac{k_2 M_1}{k_2 M_1 + k_4 R_2}, \\ z_1 &= \frac{d_1}{d}, \quad z_2 = \frac{d_2}{d}, \quad z_3 = \frac{d_3}{d}, \\ d_1 &= -(\kappa_2 M_1 + \kappa_4 R_2), \\ d_2 &= \kappa_3 - \kappa_4 R_1, \\ d_3 &= \kappa_1 - \kappa_2 R_1, \\ d &= d_1 + d_2 x_1 + d_3 x_2. \end{aligned}$$

Employing the scaling introduced via (16) to the CSP vectors given by (A6)–(A7), the scaled basis vectors $\hat{\boldsymbol{\alpha}}_r, \hat{\boldsymbol{\alpha}}_s, \hat{\mathbf{b}}_r, \hat{\mathbf{b}}_s$ obtained this time are

$$\hat{\boldsymbol{\alpha}}_r = \begin{bmatrix} 1 \\ \hat{x}_1 \\ \hat{x}_2 \end{bmatrix}, \qquad \hat{\boldsymbol{\alpha}}_s = \begin{bmatrix} -\hat{z}_2 & -\hat{z}_3 \\ 1 - \hat{x}_1 \hat{z}_2 & -\hat{x}_1 \hat{z}_3 \\ -\hat{x}_2 \hat{z}_2 & 1 - \hat{x}_2 \hat{z}_3 \end{bmatrix}, \tag{A8}$$

$$\hat{b}^r = [\hat{z}_1 \quad \hat{z}_2 \quad \hat{z}_3], \qquad \hat{b}_s = \begin{bmatrix} -\hat{x}_1 & 1 & 0 \\ -\hat{x}_2 & 0 & 1 \end{bmatrix}, \tag{A9}$$

where

$$\begin{aligned} \hat{x}_1 &= \frac{-y_3 + 8\nu\omega_2 y_2}{y_3 + 8\nu\omega_2 y_3}, \quad \hat{x}_2 = \frac{y_3}{y_3 + 8\nu\omega_2 y_2}, \\ \hat{z}_1 &= \frac{\hat{d}_1}{\hat{d}}, \quad z_2 = \frac{\hat{d}_2}{\hat{d}}, \quad z_3 = \frac{\hat{d}_3}{\hat{d}}, \\ \hat{d}_1 &= \frac{\sqrt{\kappa_2}}{\kappa_1} y_3 + \frac{8\nu\kappa_4}{\chi} y_2, \quad \hat{d}_2 = \kappa_3 - \frac{8\nu\kappa_4}{\chi} y_2, \\ \hat{d}_3 &= \kappa_1 - \sqrt{\kappa_1 \kappa_2} y_1, \quad \hat{d} = \hat{d}_1 + \hat{d}_2 \hat{x}_1 + \hat{d}_3 \hat{x}_2. \end{aligned}$$

REFERENCES

[1] A. H. Nayfeh, *Perturbation Methods*, Wiley, New York, 1973.

[2] C. M. Bender and S. A. Orszag, *Mathematical Methods for Scientists and Engineers*, McGraw-Hill, New York, 1978.

[3] P. A. Lagerstrom, *Matched Asymptotic Expansions*, Springer-Verlag, New York, 1988.

[4] I. Glassman, *Combustion*, Academic Press, New York, 1977.

[5] F. A. Williams, *Combustion Theory*, Benjamin-Cummings, Boston, 1985.

[6] N. Peters and B. Rogg, *Reduced Kinetic Mechanisms for Applications in Combustion Systems*, Springer-Verlag, Berlin, 1993.

[7] S. H. Lam and D. A. Goussis, *Conventional asymptotics and CSP for simplified kinetics modelling*, in Reduced Kinetic Mechanisms and Asymptotic Approximations for Methane-Air Flames, M. D. Smooke, ed., Springer-Verlag, Berlin, 1991.

[8] D. A. Goussis and S. H. Lam, *A study of homogeneous methanol oxidation kinetics*, in Proc. 24th Internat. Symposium on Combustion, Sydney, Australia, 1992, The Combustion Institute, Philadelphia, pp. 113–121.
[9] S. H. Lam, *Using CSP to understand complex chemical kinetics*, Combust. Sci. Tech., 89 (1993), pp. 375–404.
[10] S. H. Lam and D. A. Goussis, *The CSP method for simplifying kinetics*, Internat. J. Chem. Kinetics, 26 (1994), pp. 461–486.
[11] A. F. Trotman-Dickenson, *Gas Kinetics*, Butterworths, London 1955.
[12] S. H. Lam, *On Steady State and Partial Equilibrium Approximations for Chain Reactions*, MAE Report, Princeton University, Princeton, NJ, 1985.
[13] G. C. Hsiao and K. E. Jordan, *A numerical treatment for parabolic equations with a small parameter*, SIAM J. Math. Anal., 14 (1983), pp. 507–520.
[14] A. Jennings and J. J. McKeown, *Matrix Computation*, Wiley, London, 1992.
[15] E. S. Oran and J. P. Boris, *Numerical Simulation of Reactive Flow*, Elsevier, New York, 1987.
[16] B. A. Finlayson, *Nonlinear Analysis in Chemical Engineering*, McGraw-Hill, New York, 1980.
[17] W. H. Press, S. A. Teukolsky, W. T. Vetterling, and B. P. Flannery, *Numerical Numerical Recipes in Fortran—The Art of Scientific Computing*, Cambridge University Press, Cambridge, UK, 1992.
[18] R. D. Skeel and A. K. Kong, *Blended linear multistep methods*, ACM Trans. Math. Software 3 (1977), pp. 327–345.
[19] C. A. J. Fletcher, *Computational Techniques for Fluid Dynamics*, Springer-Verlag, Berlin, 1988.
[20] K. W. Morton and D. F. Mayers, *Numerical Solution of Partial Differential Equations*, Cambridge University Press, Cambridge, UK, 1994.